Electromagnetic currents of the pion-nucleon system

T. Skawronski,[1] B. Blankleider,[1] and A. N. Kvinikhidze[2]

[1]*School of Chemical and Physical Sciences, Flinders University, Bedford Park, South Australia 5042, Australia*
[2]*Razmadze Mathematical Institute, Tbilisi 0177, Georgia*

Pion photoproduction amplitudes are calculated from a set of equations that have been derived by coupling an external photon to all places in a dressed pion-nucleon vertex. The calculation is consistent with gauge invariance, charge conservation, unitarity, and covariance. To provide input to the photoproduction amplitude, a photon-nucleon vertex is calculated from a set of equations derived by complete attachment of photons to a dressed nucleon propagator. We check the accuracy of this vertex by extracting its nucleon electromagnetic form factors.

I. INTRODUCTION

Photons have long been used to probe the structure of nucleons and to obtain information about their excited states [1,2]. This is done by using photons to initiate various nucleon reactions, and then analyzing the results with theoretical models. Pion photoproduction is an example of such a reaction. In the literature, amplitudes for this process are calculated by using integral equations to sum up an infinite number of $\gamma N \to \pi N$ Feynman diagrams, or their nonrelativistic equivalents [3–8]. The equations used in these models are similar to the Bethe-Salpeter or Lippmann-Schwinger equations for $\pi N \to \pi N$, but with the incoming pion lines replaced with photons. Although in many cases they provide a good description of the $\gamma N \to \pi N$ data, these equations are not without difficulties. One problem is that they do not conserve electromagnetic (EM) current in a way that is theoretically correct.

Amplitudes that have gauge invariance, and hence conserve EM current, satisfy the Ward-Takahashi identity (WTI) [9,10]. This relates an $n + 1$-point function $\mathcal{G}^\mu$ that has one external photon [an example of which is the five-point function in Eq. (9)] to an n-point Green function $\mathcal{G}$ [such as the four-point function in Eq. (1)]. If $\mathcal{G}^\mu$ were evaluated exactly it would include the infinite number of diagrams that can be constructed by attaching an external photon line (EM current) to the diagrams comprising $\mathcal{G}$. Summing all these terms is extremely difficult, however, and for numerical calculations to be practical one must resort to truncating the series for $\mathcal{G}^\mu$ and $\mathcal{G}$. To preserve gauge invariance this should be done in such a way as to maintain the relationship between $\mathcal{G}^\mu$ and $\mathcal{G}$ that is specified by the WTI.

There are many ways of constructing a $\mathcal{G}^\mu$ that satisfies the WTI, but to be consistent with the exact case, $\mathcal{G}^\mu$ should include the sum of all diagrams that can be obtained by attaching a photon to the diagrams retained in the approximated $\mathcal{G}$. By using various approximations, the photoproduction amplitudes of [3–8] all satisfy the WTI, and hence achieve gauge invariance, to varying degrees. However, since the photons do not attach to the other particles in all possible ways, gauge invariance is not achieved in the correct manner.

To construct a $\gamma N \to \pi N$ amplitude that *does* achieve gauge invariance in the correct way, one can take any set of $N \to \pi N$ diagrams, write down terms for every possible way a photon could attach to them, and add them up. The gauging of equations method [11–16] allows this to be done even if we want the photoproduction amplitude to contain an infinite number of diagrams. It uses the fact that complete attachment of photons to all terms generated by an integral equation can be achieved by attaching to only a finite number of places in the integral equation itself. The result is a closed expression for a gauge invariant, nonperturbative amplitude T^μ that can be solved in a straightforward way. This amplitude also obeys Watson's theorem, and thus has unitarity.

In Sec. VII, T^μ is calculated using a covariant model of the strong interaction as input. As in Refs. [3–8], we work in the context of the traditional few-body meson theory, where the structure of mesons and baryons is described by cutoff form factors. This choice is both technically convenient and relevant to current approaches used to study nucleon resonances [17]. Similar calculations have been undertaken by Haberzettl *et al.* [18–20], but in their work the dressed photon-nucleon vertex that appears in the nucleon pole term of T^μ [first diagram on the right-hand side (RHS) of Fig. 2] was constructed by using its general analytical form as prescribed by Ball and Chiu [21,22]. By contrast, we have included in this vertex the complete sum of diagrams obtained by gauging a dressed nucleon propagator. To our knowledge, the $\gamma N \to \pi N$ calculations presented in this paper are the first in which gauge invariance is achieved through the complete attachment of photons to an infinite set of Feynman diagrams.

II. THE GAUGING OF EQUATIONS METHOD

We begin by outlining the gauging method and its application to the pion-nucleon system. Following Ref. [15], we consider the task of gauging the following four-point Green function $\mathcal{G}$ that describes interactions between point-like pions

and nucleons:

$$(2\pi)^4\delta^4(p_1' + p_2' - p_1 - p_2)\mathcal{G}(p_1', p_2', p_1, p_2)$$
$$= \int d^4y_1 d^4y_2 d^4x_1 d^4x_2 e^{i(p_1' \cdot y_1 + p_2' \cdot y_2 - p_1 \cdot x_1 - p_2 \cdot x_2)}$$
$$\times \langle\langle 0|T[\psi(y_2)\phi(y_1)\bar{\psi}(x_2)\bar{\phi}(x_1)]|0\rangle\rangle, \tag{1}$$

where ψ and ϕ are Heisenberg fields of nucleons and pions, respectively, $|0\rangle\rangle$ is the physical vacuum, and T is the time ordering operator. The x_m and y_m are the initial and final spacetime coordinates of pions ($m = 1$) and nucleons ($m = 2$), while the p_m, p_m' are their initial and final state momenta. When evaluated with Wick's theorem, $\mathcal{G}$ can be written as the sum of all possible $\pi N \to \pi N$ Feynman diagrams. In turn, these can be split into the sums of one-particle reducible (1PR) and one-particle irreducible parts as $\mathcal{G} = \mathcal{G}_{1PR} + G$.

The gauged version of G is needed in the derivation of T^μ, and we first apply the gauging method to this sum of diagrams. It can be expressed in compact form by the Bethe-Salpeter (BS) equation:

$$G(p_1', p_2', p_1, p_2)$$
$$= G_0(p_1', p_2', p_1, p_2) + \int \frac{d^4r_1}{(2\pi)^4}\frac{d^4s_1}{(2\pi)^4}G_0(p_1', p_2', r_1, r_2)$$
$$\times v(r_1, r_2, s_1, s_2)G(s_1, s_2, p_1, p_2), \tag{2}$$

where the total momentum of the pion-nucleon system is $p = p_1' + p_2' = p_1 + p_2 = s_1 + s_2 = r_1 + r_2$. In Eq. (2), G_0 is the sum of all fully disconnected $\pi N \to \pi N$ diagrams and the potential v is the sum of all amputated, connected, two-particle irreducible $\pi N \to \pi N$ diagrams. That G_0 is disconnected means it splits into two single-particle propagators g_N and g_π which are the sums of all possible $N \to N$ and $\pi \to \pi$ diagrams:

$$G_0(p_1', p_2', p_1, p_2) = (2\pi)^4\delta^4(p_1' - p_1)g_\pi(p_1)g_N(p_2). \tag{3}$$

No total momentum conservation delta function has been included in G_0 because the momenta are understood to be related in the way specified just below Eq. (2).

It is convenient to suppress the integrals and momentum labels in Eq. (2) and to write the BS equation in the shorthand notation

$$G = G_0 + G_0 v G. \tag{4}$$

In this form, the equation is reduced to a topological statement about the structure of the Feynman diagrams belonging to G. As such, it can be utilized directly to express the structure of the same Feynman diagrams, but with a photon (EM current) attached to all places in all of them. Using a superscript μ to indicate quantities that have had this attachment carried out in all possible ways, it immediately follows that

$$G^\mu = G_0^\mu + G_0^\mu v G + G_0 v^\mu G + G_0 v G^\mu, \tag{5}$$

The third term on the RHS of this equation, for instance, is shorthand for

$$\int \frac{d^4r_1}{(2\pi)^4}\frac{d^4s_1}{(2\pi)^4}G_0(k_1, k_2, s_1, s_3)$$
$$\times v^\mu(s_1, s_2, r_1, r_2)G(r_1, r_2, p_1, p_2). \tag{6}$$

The total momentum to the right of the attachment point is $p = p_1 + p_2 = r_1 + r_2$ and that to the left is $p + q = s_1 + s_2 = k_1 + k_2$. The momentum q is that transferred to the particles during the attachment.

Equation (5) expresses the gauged version of G^μ in terms of an integral equation and illustrates what is meant by "gauging an equation." Both G^μ and G_0^μ are obtained from G and G_0 but with a photon attached to all possible places in all diagrams contributing to them. The gauged potential v^μ is similarly obtained from v, but because v consists of amputated diagrams, v^μ does not include terms that can be obtained by attaching to their external legs. Notice that the final three terms in Eq. (5) can also be expressed as $[G_0 v G]^\mu$, which illustrates a rule for the gauging of products that is identical to the product rule for derivatives.

Some simple algebra allows Eq. (5) to be formally solved, giving

$$G^\mu = -G[G^{-1}]^\mu G = G[G_0^{-1}G_0^\mu G_0^{-1} + v^\mu]G, \tag{7}$$

where, in longhand, the inverse of G_0 is

$$G_0^{-1}(p_1', p_2', p_1, p_2) = (2\pi)^4\delta^4(p_1' - p_1)g_\pi^{-1}(p_1)g_N^{-1}(p_2). \tag{8}$$

The terms that make up the single-particle propagators can also be generated by integral equations, allowing G_0 to be gauged in a similar way to G. This is done in Sec. II B.

A. The Ward-Takahashi identity

To verify that the diagrams comprising G^μ come in the right combination to preserve gauge invariance, let us suppose that instead of constructing a five-point function by gauging, it is found by evaluating

$$\mathcal{G}_{\text{Exact}}^\mu(k_1, k_2, p_1, p_2)$$
$$= \int d^4y_1 d^4y_2 d^4x_1 d^4x_2 e^{i(k_1 \cdot y_1 + k_2 \cdot y_2 - p_1 \cdot x_1 - p_2 \cdot x_2)}$$
$$\times \langle\langle 0|T[\psi(y_2)\phi(y_1)\bar{\psi}(x_2)\bar{\phi}(x_1)J^\mu(0)]|0\rangle\rangle \tag{9}$$

where the initial and final state momenta are related to each other the same way as in expression (6). The EM current J^μ corresponds to a phase transformation of the charged particle fields. The generators of this transformation are

$$\lambda_N = \frac{e}{2}(1 + \tau_3), \quad \lambda_{\pi ba} = ie\epsilon_{b3a}, \tag{10}$$

where τ_3 is the Pauli matrix for the third component of isospin, ϵ_{b3a} is the Levi-Civita symbol, and $e = \sqrt{4\pi/137}$ is the elementary charge. The a and b subscripts on λ_π label the pion charges.

For the EM current to be conserved it must satisfy the condition $\partial_\mu J^\mu = 0z$, and this, in turn, results in $\mathcal{G}_{\text{Exact}}^\mu$ satisfying the two-body WTI [10]:

$$-iq_\mu\mathcal{G}_{\text{Exact}}^\mu(k_1, k_2, p_1, p_2)$$
$$= \lambda_\pi\mathcal{G}(k_1 - q, k_2, p_1, p_2) + \lambda_N\mathcal{G}(k_1, k_2 - q, p_1, p_2)$$
$$- \mathcal{G}(k_1, k_2, p_1 + q, p_2)\lambda_\pi - \mathcal{G}(k_1, k_2, p_1, p_2 + q)\lambda_N, \tag{11}$$

To simplify this expression, the pion charge labels have been left off.

The Feynman diagrams that comprise $\mathcal{G}^\mu_{\text{Exact}}$ come in two types. The first type, $\mathcal{G}^\mu$, can be constructed by attaching photons to the Feynman diagrams that make up $\mathcal{G}$. Diagrams of the second type cannot be constructed in this way, but vanish when they are contracted with q_μ and so do not contribute to the WTI. The diagrams that make up $\mathcal{G}^\mu$ may be further sorted into two sets, $\mathcal{G}^\mu_{\text{1PR}}$ and G^μ, according to whether they can be obtained by attaching photons to $\mathcal{G}_{\text{1PR}}$ or G. Thus $\mathcal{G}^\mu_{\text{1PR}}$ and G^μ must satisfy separate WTIs that add up to identity (11). These are the same as the WTI for $\mathcal{G}^\mu$, but involve G^μ, G and $\mathcal{G}^\mu_{\text{1PR}}$, $\mathcal{G}_{\text{1PR}}$ instead. It is easy to show that the G^μ of Eq. (7) satisfies the appropriate WTI provided that v^μ satisfies

$$
\begin{aligned}
-i q_\mu & v^\mu_{lj}(k_1, k_2, p_1, p_2) \\
= & \lambda_{\pi l m} v_{mj}(k_1 - q, k_2, p_1, p_2) + \lambda_N v_{lj}(k_1, k_2 - q, p_1, p_2) \\
& - v_{lm}(k_1, k_2, p_1 + q, p_2)\lambda_{\pi m j} \\
& - v_{lj}(k_1, k_2, p_1, p_2 + q)\lambda_N
\end{aligned}
\tag{12}
$$

and G^μ_0 obeys an identity the same as Eq. (11) but involving G^μ_0 and G_0 instead.

To obtain an expression for G^μ_0, we can use the product rule to write

$$
\begin{aligned}
G^\mu_0(k_1, k_2, p_1, p_2) = & (2\pi)^4 \delta^4(k_1 - p_1) g^\mu_N(k_2, p_2) g_\pi(k_1) \\
& + (2\pi)^4 \delta^4(k_2 - p_2) g_N(k_2) g^\mu_\pi(k_1, p_1),
\end{aligned}
\tag{13}
$$

where it is understood that $k_1 + k_2 = p_1 + p_2 + q$. Deriving G^μ_0 is thus a matter of gauging the single-particle propagators. This we do in the next section.

B. Gauge invariant $\gamma N \rightarrow N$ vertex

In what follows it is assumed that the interaction of pions and nucleons is described by an interaction Lagrangian linear in the pion field. We shall, however, neglect explicit dressings of pions. Consequently, g_π is a Feynman propagator for a meson with mass $m_\pi \approx 138$ MeV:

$$
g_\pi(k) = \frac{i}{k^2 - m^2_\pi + i\epsilon}.
\tag{14}
$$

Meanwhile, the sum of diagrams comprising the dressed nucleon propagator g_N can be represented by the Dyson-Schwinger equation,

$$
g_N(p) = g_{N0}(p) + g_{N0}(p)\Sigma_N(p)g_N(p),
\tag{15}
$$

where the nucleon self energy Σ_N is the sum of all $N \rightarrow N$ diagrams that are one-particle irreducible. The "bare" nucleon propagator g_{N0} is a Feynman propagator for a fermion with mass m_{N0}:

$$
g_{N0}(p) = \frac{i}{\not{p} - m_{N0} + i\epsilon}.
\tag{16}
$$

We refer to m_{N0} as the bare nucleon mass and it is set so that g_N has a pole at $p_0 = m_N \approx 939$ MeV in the nucleon rest frame. As discussed in detail in Appendix A, we express the

dressed nucleon propagator in terms of positive and negative energy components as

$$
-i g_N(p) = \Lambda^+ g^+_N(p_0) + \Lambda^- g^-_N(p_0),
\tag{17}
$$

where $\Lambda^\pm = \frac{1}{2}(1 \pm \gamma_0)$. The residue of $g^+_N(p_0)$ at $p_0 = m_N$ is called the renormalization constant Z_2, and this is calculated in Sec. III.

Equation (15) has the same form as the BS equation for G, so gauging g_N gives

$$
\begin{aligned}
g^\mu_N = & -g_N[g^{-1}_N]^\mu g_N = g_N \Gamma^\mu_N g_N, \\
\Gamma^\mu_N = & \Gamma^\mu_{N0} + \Sigma^\mu_N, \quad g^\mu_{N0} = g_{N0}\Gamma^\mu_{N0}g_{N0}.
\end{aligned}
\tag{18}
$$

By analogy with the WT identities written above, g^μ_{N0} and g^μ_π should satisfy

$$
\begin{aligned}
-i q_\mu g^\mu_{N0}(p', p) = & \lambda_N g_{N0}(p) - g_{N0}(p')\lambda_N, \\
-i q_\mu g^\mu_\pi(k', k) = & \lambda_\pi g_\pi(k) - g_\pi(k')\lambda_\pi.
\end{aligned}
\tag{19}
$$

The gauged pion propagator may also be written as $g^\mu_\pi = g_\pi \Gamma^\mu_\pi g_\pi$, and it is easy to verify that the bare vertices

$$
\begin{aligned}
\Gamma^\mu_{N0} = & \lambda_N \gamma^\mu, \\
\Gamma^\mu_\pi(k', k) = & \lambda_\pi(k'^\mu + k^\mu)
\end{aligned}
\tag{20}
$$

allow g^μ_π and g^μ_{N0} to satisfy (19). Note that these vertices differ from those specified by Feynman rules (see, for example, Appendix A of [23]) by a factor of $-i$. Thus the quantities we derive by gauging need to be multiplied by $-i$ to make them consistent with Feynman rules.

To gauge the infinite number of diagrams that make up the self-energy, we note that they can be expressed as

$$
\begin{aligned}
\Sigma_N(p) = \int & \frac{d^4 r}{(2\pi)^4} \frac{d^4 s}{(2\pi)^4} \bar{f}^a_0(k, p, p - r) \\
& \times G_0(r, p - r, s, p - s)f^a(s, p - s, p).
\end{aligned}
\tag{21}
$$

The bare pion absorption vertex $\bar{f}_0$ may be read directly from the Lagrangian, while the dressed pion emission vertex f is given by the integral equation

$$
\begin{aligned}
f^a(k, p - k, p) = & f^a_0(k, p - k, p) \\
& + \int \frac{d^4 r}{(2\pi)^4} \frac{d^4 s}{(2\pi)^4} v_{ab}(k, p - k, r, p - r) \\
& \times G_0(r, p - r, s, p - s)f^b(s, p - s, p).
\end{aligned}
\tag{22}
$$

It is convenient to express the above two equations in the shorthand form

$$
\begin{aligned}
\Sigma_N = & \bar{f}_0 G_0 f = \bar{f}_0 G f_0, \\
f = & f_0 + v G_0 f.
\end{aligned}
\tag{23}
$$

Applying the product rule then yields the gauged self-energy

$$
\Sigma^\mu_N = \bar{f} G^\mu_0 f + \bar{f} G_0 f^\mu_0 + \bar{f}^\mu_0 G_0 f + \bar{f} G_0 v^\mu G_0 f.
\tag{24}
$$

The vertex that results from using this in Γ^μ_N is illustrated in Fig. 1. The gauged bare vertices f^μ_0, $\bar{f}^\mu_0$ are model dependent, and expressions for these are not given until Sec. V. We can,
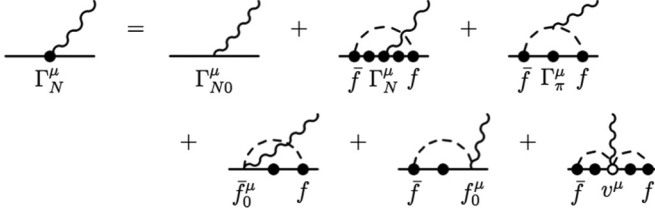
FIG. 1. The photon-nucleon vertex of Eq. (18). The dashed, solid, and wiggly lines denote pions, nucleons, and photons, respectively.

however, say that since f_0 is an amputated quantity, its gauged version needs to satisfy a WTI analogous to (12)

$$
\begin{aligned}
-iq_\mu f_0^{\mu a}(k, p'-k, p) =\ & \lambda_N f_0^a(k, p'-k-q, p) \\
& + \lambda_{\pi ab} f_0^b(k-q, p'-k, p) \\
& - f_0^a(k, p'-k, p')\lambda_N.
\end{aligned}
\tag{25}
$$

Meanwhile, since g_{N0}^μ satisfies (19), one would expect g_N^μ to have the WTI

$$
-iq_\mu g_N^\mu(p+q, p) = \lambda_N g_N(p) - g_N(p+q)\lambda_N.
\tag{26}
$$

By putting the preceding two WTIs into $q_\mu \Gamma_N^\mu$, it is easy to recover Eq. (26). Therefore, provided f_0^μ and v^μ are constructed such that they satisfy the appropriate WTIs, g_N^μ constitutes a gauge invariant description of $\gamma N \to N$. It then immediately follows that the G_0^μ found by gauging satisfies a WTI the same as Eq. (11) but with G_0^μ and G_0 substituted for $\mathcal{G}^\mu$ and $\mathcal{G}$.

Since there exist data for the process described by g_N^μ, this quantity can be compared with experiment. First, though, the external legs of its constituent Feynman diagrams need to be "amputated." This involves removing each external g_π, and replacing each external g_N with a factor of $\sqrt{Z_2}$. We also adopt a convention whereby amplitudes are multiplied by an extra factor of i that cancels the $-i$ needed to convert gauged quantities to Feynman diagrams. The properly normalized photon-nucleon vertex is therefore

$$
\Gamma_Z^\mu = Z_2 \Gamma_N^\mu.
\tag{27}
$$

C. Gauge invariant description of $\gamma N \to \pi N$

A gauge invariant amplitude for $\gamma N \to \pi N$ may be derived by applying the gauging method to the unamputated πNN vertex $\mathcal{F} = G_0 f g_N = G f_0 g_N$. The result, illustrated in Fig. 2, is given by

$$
\mathcal{F}^\mu = G_0 T^\mu g_N,
\tag{28}
$$

where

$$
\begin{aligned}
T^\mu =\ & v_u^\mu + v_t^\mu + v_s^\mu + tG_0^\mu f + tG_0 v^\mu G_0 f \\
& + tG_0 f_0^\mu + f_0^\mu + v^\mu G_0 f,
\end{aligned}
\tag{29a}
$$

$$
t = v + vG_0 t,
\tag{29b}
$$

$$
v_t^{\mu a} = \Gamma_\pi^\mu(k_f, k_f - q)g_\pi(k_f - q)f^a(k_f - q, p_f, p_i),
\tag{29c}
$$

$$
v_u^{\mu a} = \Gamma_N^\mu(p_f, p_f - q)g_N(p_f - q)f^a(k_f, p_f - q, p_i),
\tag{29d}
$$

$$
v_s^{\mu a} = f^a(k_f, p_f, p_i + q)g_N(p_i + q)\Gamma_N^\mu(p_i + q, p_i).
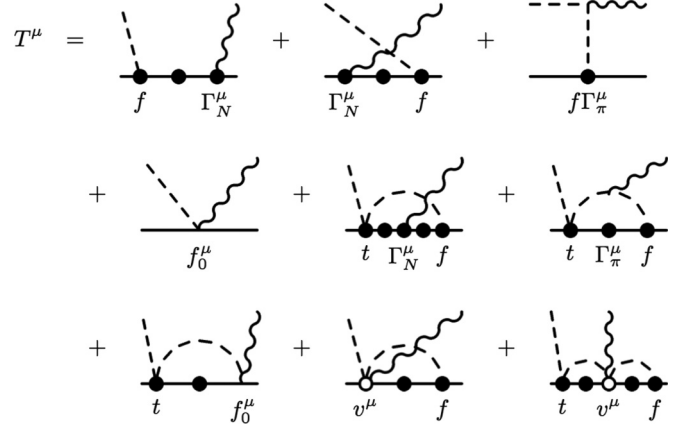\tag{29e}
$$

FIG. 2. The singly gauged amplitude of Eq. (29a).

In writing Eq. (28), use has been made of the fact that $G_0^{-1}G = 1 + tG_0$. The v^μ's in equations (29) are, like T^μ, all functions of k_f, p_f, p_i. The a index, which labels the charge of the emitted pion, has also been dropped in many instances in order to simplify the notation.

When the inputs v^μ, f_0^μ, g_N^μ, and G_0^μ satisfy the Ward-Takahashi identities written thus far in this section, the amplitude $\mathcal{F}^\mu$ is also gauge invariant. It obeys the following WTI:

$$
\begin{aligned}
-iq_\mu \mathcal{F}^{\mu a}(k_f, p_f, p_i) =\ & \lambda_{\pi ab} \mathcal{F}^b(k_f - q, p_f, p_i) \\
& + \lambda_N \mathcal{F}^a(k_f, p_f - q, p_i) \\
& - \mathcal{F}^a(k_f, p_f, p_i + q)\lambda_N.
\end{aligned}
\tag{30}
$$

The singly gauged amplitude is also consistent with two-body unitarity. To see this, we need only note that T^μ can be rearranged into a form similar to the Bethe-Salpeter and Lippmann-Schwinger equations:

$$
\begin{aligned}
T^\mu &= V^\mu + T G_0 V^\mu, \\
V^\mu &= v^\mu G_0 f + f_0^\mu + \Gamma_\pi^\mu g_\pi f + f_0 g_{N0} \Gamma_{N0}^\mu \\
&\quad + \Gamma_N^\mu g_N f + f_0 g_{N0} \bar{f}_0^\mu G_0 f, \\
T &= t + f g_N \bar{f}.
\end{aligned}
\tag{31}
$$

In other words, T^μ has the same form as the amplitudes in [3–8]. Since they all have two-body unitarity, it immediately follows that T^μ does as well.

Upon amputating the external legs from $\mathcal{F}^\mu$, we arrive at the following properly normalized singly gauged amplitude which incorporates gauge invariance and unitarity:

$$
T_Z^{\mu a} = Z_2 T^{\mu a}.
\tag{32}
$$

III. NUCLEON RESONANCES

In this section, the equations for Γ_Z^μ and $T_Z^{\mu a}$ are extended to include contributions from excited state nucleons. The lowest energy excited state is the $\Delta(1232)$ particle, which has spin and isospin both equal to 3/2. However, the lowest order $\gamma N \to \pi N$ diagram involving the Δ, which is shown in Fig. 3, cannot be obtained by gauging because the diagram that results from removing the incoming photon does not
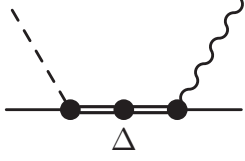
FIG. 3. Diagram needed to describe certain $\gamma N \to \pi N$ data that cannot be obtained by gauging.

exist. This is not a deficiency of the gauging method, though, because the diagram is gauge invariant on its own and can be added on to T^μ without violating the WTI.

Another excited state of relative importance is the $N^*(1440)$ Roper resonance. This has the same spin and isospin as the ground state nucleon, and if the Δ particle in the intermediate state of Fig. 3 is replaced by a Roper, the result is a class of diagrams that are not self gauge invariant, but which *can* be obtained by gauging. This is done in Secs. III A and III B.

Following the $\pi N \to \pi N$ models of [24,25], we suppose that the Roper resonance occurs in one-particle states only. For πN scattering, this situation may be described by the properly normalized "coupled channels" amplitude $\mathcal{T}$ given by

$$\mathcal{T} = iZ_2 t + iZ_2 \sum_{\alpha\beta} f_\beta g_{\beta\alpha} \bar{f}_\alpha,$$

$$f_\alpha = f_{\alpha 0} + t G_0 f_{\alpha 0}, \quad \bar{f}_\alpha = \bar{f}_{\alpha 0} + \bar{f}_{\alpha 0} G_0 t, \quad (33)$$

$$\Sigma_{\alpha\beta} = \bar{f}_{\alpha 0} G_0 f_\beta, \quad g_{\alpha\beta} = g_{\alpha 0}\delta_{\alpha\beta} + \sum_\rho g_{\alpha 0} \Sigma_{\alpha\rho} g_{\rho\beta},$$

where the subscripts α, β, ρ can be N (for a nucleon) or R (for a Roper particle). The bare Roper propagator g_{R0} is the same as g_{N0} but with the bare Roper mass m_{R0} substituted for m_{N0}. As discussed in detail in Appendix A, the elements $g_{\alpha\beta}$ of the 2×2 matrix $\boldsymbol{g}$ are given explicitly as

$$\boldsymbol{g} = \begin{pmatrix} g_R^{-1}/\Delta & \Sigma_{NR}/\Delta \\ \Sigma_{NR}/\Delta & g_N^{-1}/\Delta \end{pmatrix} = \begin{pmatrix} g_{NN} & g_{NR} \\ g_{RN} & g_{RR} \end{pmatrix}, \quad (34)$$

where $\Delta = g_N^{-1} g_R^{-1} - \Sigma_{NR}^2$ is the determinant of $\boldsymbol{g}^{-1}$. The "no baryon mixing" Roper propagator g_R is given by an expression the same as (15) but with g_{R0} and Σ_{RR} in place of g_{N0} and $\Sigma_N \equiv \Sigma_{NN}$, respectively.

When working in the center-of-mass frame where the total momentum is $p = (p_0, \boldsymbol{0})$, the positive energy part of $\boldsymbol{g}$ can be isolated by writing it as

$$-i\boldsymbol{g}(p) = \boldsymbol{g}^+(p_0)\Lambda^+ + \boldsymbol{g}^-(p_0)\Lambda^-. \quad (35)$$

In the coupled channels system, the elements of $\boldsymbol{g}^+$ need to have poles at m_N and the Roper mass $m_R \approx 1365 - 95i$ MeV. To arrange this, the denominator

$$\Delta^+ = [g_N^{-1}]^+ [g_R^{-1}]^+ - [\Sigma_{NR}^+]^2 \quad (36)$$

must vanish when $p_0 = m_N$ or $p_0 = m_R$. The quantities on the RHS of Eq. (36) are defined by

$$ig_\beta^{-1}(p) = \Lambda^+ [g_\beta^+(p_0)]^{-1} + \Lambda^- [g_\beta^-(p_0)]^{-1},$$

$$i\Sigma(p) = \Sigma^+(p_0)\Lambda^+ + \Sigma^-(p_0)\Lambda^-. \quad (37)$$

Setting $\Delta^+(m_N) = \Delta^+(m_R) = 0$ gives us a pair of simultaneous equations that can be solved to find the required bare masses, and we get

$$m_{\alpha 0} = \frac{1}{2\mathcal{A}_\alpha}\left(-\mathcal{B}_\alpha \pm \sqrt{\mathcal{B}_\alpha^2 - 4\mathcal{A}_\alpha \mathcal{C}_\alpha}\right), \quad (38)$$

where

$$\mathcal{A}_\alpha = a_{\beta\beta} - a_{\beta\alpha},$$
$$\mathcal{B}_\alpha = (a_{\beta\alpha} - a_{\beta\beta})(a_{\alpha\beta} + a_{\alpha\alpha}) - c_\alpha + c_\beta,$$
$$\mathcal{C}_\alpha = a_{\alpha\alpha} a_{\alpha\beta}(a_{\beta\beta} - a_{\beta\alpha}) - a_{\alpha\alpha} c_\alpha + a_{\alpha\beta} c_\alpha,$$
$$a_{\alpha\beta} = m_\beta - \Sigma_{\alpha\alpha}^+(m_\beta), \quad c_\alpha = [\Sigma_{NR}^+(m_\alpha)]^2. \quad (39)$$

In the first three lines of Eq. (39), $\beta = R$ if $\alpha = N$ and vice versa. Meanwhile, the signs in Eq. (38) need to be chosen so that it reduces to $[d_R^+(m_R)]^{-1} = 0$ and $[d_N^+(m_N)]^{-1} = 0$ when $\Sigma_{NR} \to 0$ and hence there is no mixing of the ground and excited states.

When calculating $\Sigma^+(m_R)$, one needs to take into account that because Σ^+ is a function of $p_0 = \sqrt{p^2}$, it has two possible values at each point in the complex p^2 plane. To make it a single-valued function, the p^2 plane can be replaced by a Riemann surface consisting of two sheets [26,27]. Σ^+ contributes a cut to the p^2 plane running just below the real axis from $(m_N + m_\pi)^2 - i\epsilon$ to $\infty - i\epsilon$, and the two sheets can be joined along this cut so that passing through it takes us from one sheet to the other. Then a particular p^2 value is on the first sheet if $0 \leqslant \arg(p^2) < 2\pi$ and on the second if $2\pi \leqslant \arg(p^2) < 4\pi$. We must place m_R^2 on the second sheet when calculating $\Sigma^+(m_R)$ because an m_R^2 on the first sheet has $\sqrt{m_R^2} = -m_R$. This can be done by rotating the loop integral contour such that the cut in the p^2 plane passes clockwise over m_R^2 and ends up at some angle in between the positive real axis and the negative imaginary axis. This rotation is discussed further in Sec. IV.

One must also ensure that the pion-nucleon interaction described by f_α has the correct strength. To do this the model parameters should be adjusted such that the pion-nucleon coupling constant $g_{\pi NN}$, an expression for which is given in Appendix D, has its experimental value of 13.02.

In evaluating $g_{\pi NN}$, a coupled channels renormalization constant needs to be calculated by taking the residue of $\boldsymbol{g}^+(p_0)$ at $p_0 = m_N$. Because $\Sigma_{NR}^+(m_N) = [g_R^+(m_N)]^{-1}[g_N^+(m_N)]^{-1}$, this residue can be factorized into the product of a row matrix and its transpose. The "square root" of the renormalizsation constant in the coupled channels system is thus either 1×2 or 2×1:

$$\operatorname*{Res}_{p_0=m_N} \boldsymbol{g}^+(p_0) = \begin{pmatrix} \sqrt{Z_N} \\ \sqrt{Z_R} \end{pmatrix}\begin{pmatrix} \sqrt{Z_N} & \sqrt{Z_R} \end{pmatrix}. \quad (40)$$

The elements are given by

$$Z_\alpha = \frac{[g_\beta^+(m_N)]^{-1}}{\Delta^{+\prime}(m_N)}, \quad (41)$$

where $\beta = R$ if $\alpha = N$ and vice versa. The prime on Δ^+ in Eq. (41) denotes a derivative with respect to p_0. Note

that when $\Sigma_{NR} \to 0$ we have $[g_N^+(m_N)]^{-1} \to 0$ and the usual textbook renormalisation constant is recovered:

$$Z_N \to Z_2 = \left[\frac{d}{dp_0} [g_N^+(p_0)]^{-1} \Big|_{p_0=m_N} \right]^{-1} \tag{42}$$

A. Gauge invariant, coupled channels description of $\gamma N \to N$

To obtain a gauge invariant, coupled channels $\gamma N \to N$ vertex, we repeat the process described in Sec. II B but with the ordinary numbers replaced by matrices. Doing this, we obtain

$$\boldsymbol{g}^\mu = -\boldsymbol{g}[\boldsymbol{g}^{-1}]^\mu \boldsymbol{g} = \boldsymbol{g} \begin{pmatrix} -[g_N^{-1}]^\mu & \Sigma_{NR}^\mu \\ \Sigma_{RN}^\mu & -[g_R^{-1}]^\mu \end{pmatrix} \boldsymbol{g}. \tag{43}$$

The matrix between the factors of $\boldsymbol{g}$ on the RHS will be denoted as $\boldsymbol{\Gamma}^\mu$. Its elements are given by expressions the same as those in Eqs. (18) and (24) but with different vertices at the edges of the pion loops:

$$\Gamma_\alpha^\mu = -[g_\alpha^{-1}]^\mu = \Gamma_{\alpha 0}^\mu + \Sigma_{\alpha\alpha}^\mu, \tag{44a}$$

$$\Sigma_{\beta\alpha}^\mu = \bar{f}_{\beta 0}^\mu G_0 f_\alpha + \bar{f}_\beta G_0^\mu f_\alpha + \bar{f}_\beta G_0 v^\mu G_0 f_\alpha + \bar{f}_\beta G_0 f_{\alpha 0}^\mu. \tag{44b}$$

We have chosen the bare Roper vertex Γ_{R0}^μ to be the same as the bare nucleon vertex in Eq. (20).

As was the case for g_N^μ, the external propagators need to be amputated from $\boldsymbol{g}^\mu$ before it can be compared with experimental data. That is, the external propagators must be removed and the result multiplied from the left and right by the 1×2 and 2×1 renormalization constants. Thus the properly normalized coupled channels vertex is

$$\Gamma_Z^\mu = \begin{pmatrix} \sqrt{Z_N} & \sqrt{Z_R} \end{pmatrix} \begin{pmatrix} -[g_N^{-1}]^\mu & \Sigma_{NR}^\mu \\ \Sigma_{RN}^\mu & -[g_R^{-1}]^\mu \end{pmatrix} \begin{pmatrix} \sqrt{Z_N} \\ \sqrt{Z_R} \end{pmatrix}. \tag{45}$$

B. Gauge invariant, coupled channels description of $\gamma N \to \pi N$

As the present model has Roper particles appearing only in one body states, the task of deriving a singly gauged amplitude that includes Roper contributions is a matter of gauging $\mathcal{F} = G_0 \boldsymbol{f} \boldsymbol{g} = G \boldsymbol{f}_0 \boldsymbol{g}$, where

$$\boldsymbol{f} = (f_N \quad f_R), \qquad \boldsymbol{f}_0 = (f_{N0} \quad f_{R0}). \tag{46}$$

The product rule yields an expression for $\mathcal{F}^\mu$ that is very similar to Eq. (28):

$$\mathcal{F}^\mu = G_0 \boldsymbol{T}^\mu \boldsymbol{g}, \tag{47}$$

where

$$\boldsymbol{T}^\mu = \boldsymbol{v}_u^\mu + \boldsymbol{v}_t^\mu + \boldsymbol{v}_s^\mu + t G_0^\mu \boldsymbol{f} + t G_0 v^\mu G_0 \boldsymbol{f} + t G_0 \boldsymbol{f}_0^\mu + \boldsymbol{f}_0^\mu + v^\mu G_0 \boldsymbol{f} \tag{48}$$

and

$$\boldsymbol{v}_t^{\mu a} = \Gamma_\pi^\mu(k_f, k_f - q) g_\pi(k_f - q) \boldsymbol{f}^a(k_f - q, p_f, p_i), \tag{49a}$$

$$\boldsymbol{v}_u^{\mu a} = \Gamma_N^\mu(p_f, p_f - q) g_N(p_f - q) \boldsymbol{f}^a(k_f, p_f - q, p_i), \tag{49b}$$

$$\boldsymbol{v}_s^{\mu a} = \boldsymbol{f}^a(k_f, p_f, p_i + q) \boldsymbol{g}(p_i + q) \boldsymbol{\Gamma}^\mu(p_i + q, p_i). \tag{49c}$$

The gauged matrix vertex $\boldsymbol{f}_0^{\mu a}$ is the same as $\boldsymbol{f}_0^a$, but with $f_{N0}^{\mu a}, f_{R0}^{\mu a}$ substituted for f_{N0}^a, f_{R0}^a. To allow the g_N inside G_0 to have a nucleon pole, the bare mass inside the two-body propagator G_0 is taken to be different from that in $\boldsymbol{g}$. Thus, amputating the external legs of $\mathcal{F}^\mu$ now involves removing the external propagators, multiplying from the right by the 2×1 renormalization constant and from the left by $\sqrt{Z_2}$:

$$T_Z^{\mu a} = \sum_\rho \sqrt{Z_2} T_\rho^{\mu a} \sqrt{Z_\rho} \tag{50}$$

IV. STRONG INTERACTION MODEL

To provide the necessary input to a calculation of Γ_Z^μ and $T_Z^{\mu a}$, the bare vertices $f_{\alpha 0}$ and the potential v need to specified. Rather than developing a new model for these, we have borrowed from the covariant $\pi N \to \pi N$ description due to Gross and Surya (GS) [25], which is based on Eqs. (33). In common with most other models that use these and similar equations, the two-particle intermediate states are simplified by replacing G_0 with bare, physical mass propagators multiplied by Z_2. The factor of Z_2 causes the approximated propagator to have the same nucleon pole residue as its exact counterpart. To further reduce technical complexities, GS chose a separable v and used the spectator approach to reduce all loop integrals to three dimensions.

GS implemented the spectator approach by placing intermediate pions on shell. They were led to this choice by a careful assessment of pole contributions to typical Feynman diagrams contributing to πN scattering. However, when we used this approximation to calculate Γ_Z^μ, it was found to produce EM form factors that vary only slightly with the squared photon momentum. To overcome this problem, we carried out the spectator approach by putting the intermediate nucleons on shell instead. This amounts to making the replacement

$$G_0(k', r', k, r) \to (2\pi)^4 \delta^4(k' - k) Z_2 \frac{\pi}{E_r} i(r\!\!\!/ + m_N)$$
$$\times \frac{\delta^+(r^2 - m_N^2)}{(p_0 - E_r + \omega_k - i\epsilon)(p_0 - E_r - \omega_k + i\epsilon)}, \tag{51}$$

where $p = k + r = k' + r'$ and $E_r = \sqrt{\boldsymbol{r}^2 + m_N^2}$. Despite this change, we retained the cutoff factors, bare pion vertices, and background potential of the GS paper. The cutoff factors are

$$h_\alpha(k^2) = \left[\frac{(\Lambda_\alpha^2 - \tilde{m}_\alpha^2)^2}{(\Lambda_\alpha^2 - \tilde{m}_\alpha^2)^2 + (\tilde{m}_\alpha^2 - k^2)^2} \right]^2. \tag{52}$$

Ground state nucleons and pions have $\tilde{m}_N = m_N$, $\tilde{m}_\pi = m_\pi$ while $\tilde{m}_R$ and the cutoff masses $\Lambda_N, \Lambda_\pi, \Lambda_R$ are treated as free parameters. The bare vertices each have a factor of $\sqrt{Z_2}$ absorbed into them, and are related to the vertices of Sec. II by $\Gamma_{\alpha 0}^{\pi a} = \sqrt{Z_2} f_{\alpha 0}^a$, $\bar{\Gamma}_{\alpha 0}^{\pi a} = \sqrt{Z_2} \bar{f}_{\alpha 0}^a$. They are given by

$$\bar{\Gamma}_{\alpha 0}^{\pi a}(k, p', p) = g_{\pi N\alpha}^{(0)} \tau_a \gamma_5 (x_\alpha - y_\alpha \, k\!\!\!/) F_\alpha(k^2, p^2, p'^2),$$
$$\Gamma_{\alpha 0}^{\pi a}(k, p', p) = g_{\pi N\alpha}^{(0)} \tau_a^* (x_\alpha - y_\alpha \, k\!\!\!/) \gamma_5 F_\alpha(k^2, p'^2, p^2), \tag{53}$$

TABLE I. Parameters that were adjusted to fit the $j = 1/2$ phase shift data. The cutoff masses are in units of MeV, as is $\tilde{m}_R$. The other parameters are dimensionless.

	A	B
Λ_N	1432.99924	1358.45006
Λ_R	1948.45836	1943.97350
Λ_π	582.51508	582.61099
x_N	0.17775	0.06548
x_R	0.79282	0.87960
$g_{\pi NN}^{(0)}$	10.99164	13.44624
$g_{\pi NR}^{(0)}$	12.13224	10.70639
$\tilde{m}_R$	1449.48265	1455.25030

where

$$F_\alpha(k^2, r'^2, r^2) = h_\alpha(r^2) F_V(k^2, r'^2),$$
$$F_V(k^2, r^2) = h_\pi(k^2) h_N(r^2), \tag{54}$$

and $y_\alpha = (1 - x_\alpha)/(2m_N)$. The asterisk on the Pauli matrix in $\Gamma_{\alpha 0}^{\pi a}$ denotes a Hermitian conjugate, while $g_{\pi N\alpha}^{(0)}$ is the bare coupling constant. The extent to which the pion-nucleon coupling is pseudoscalar and pseudovector is governed by x_α, which is a number between 0 and 1.

Similar to the bare vertices, the GS background potential incorporates a factor of iZ_2 and is related to the potential written above by $iZ_2 v_{ba} = \mathcal{V}_{ba}$. It has the following form:

$$\mathcal{V}_{ba} = \mathcal{V}_{1/2}(P_{1/2})_{ba} + \mathcal{V}_{3/2}(P_{3/2})_{ba}, \tag{55}$$

where

$$\mathcal{V}_t(k', r', k, r) = F_V(k'^2, r'^2) \tilde{\mathcal{V}}_t(p) F_V(k^2, r^2),$$
$$\tilde{\mathcal{V}}_t(p) = C_0^t(p^2) \not{p} + C_1^t, \tag{56}$$

and $p = k' + r' = k + r$. The isospin projection operators are

$$(P_{1/2})_{ba} = \tfrac{1}{3} \tau_b^* \tau_a,$$
$$(P_{3/2})_{ba} = \delta_{ba} - \tfrac{1}{3} \tau_b^* \tau_a, \tag{57}$$

while the C factors are written down in Appendix B.

To set the parameters, $\pi N \to \pi N$ phase shifts were calculated from the renormalized amplitude $\mathcal{T}_{ba}(k_f, p_f, k_i, p_i)$ using the formulas given in Appendix C 1. The best set of parameters we could find when using replacement (51) are listed as Fit A in Table I and produce the phase shifts shown in Fig. 4. The horizontal axes of these graphs show the pion laboratory energies E_π, which are related to the total momentum $p = k_f + p_f = k_i + p_i$ by

$$E_\pi = \frac{p^2 - m_\pi^2 - m_N^2}{2m_N} - m_\pi. \tag{58}$$

To facilitate calculation of the bare Roper mass, m_R^2 has been placed on the second sheet of the Riemann surface discussed in Sec. III. In the center-of-mass frame, where $p = (p_0, \mathbf{0})$, the factor $[p_0 - \omega_k - E_r + i\epsilon]^{-1}$ on the RHS of replacement (51) causes a cut in the p^2 plane running from
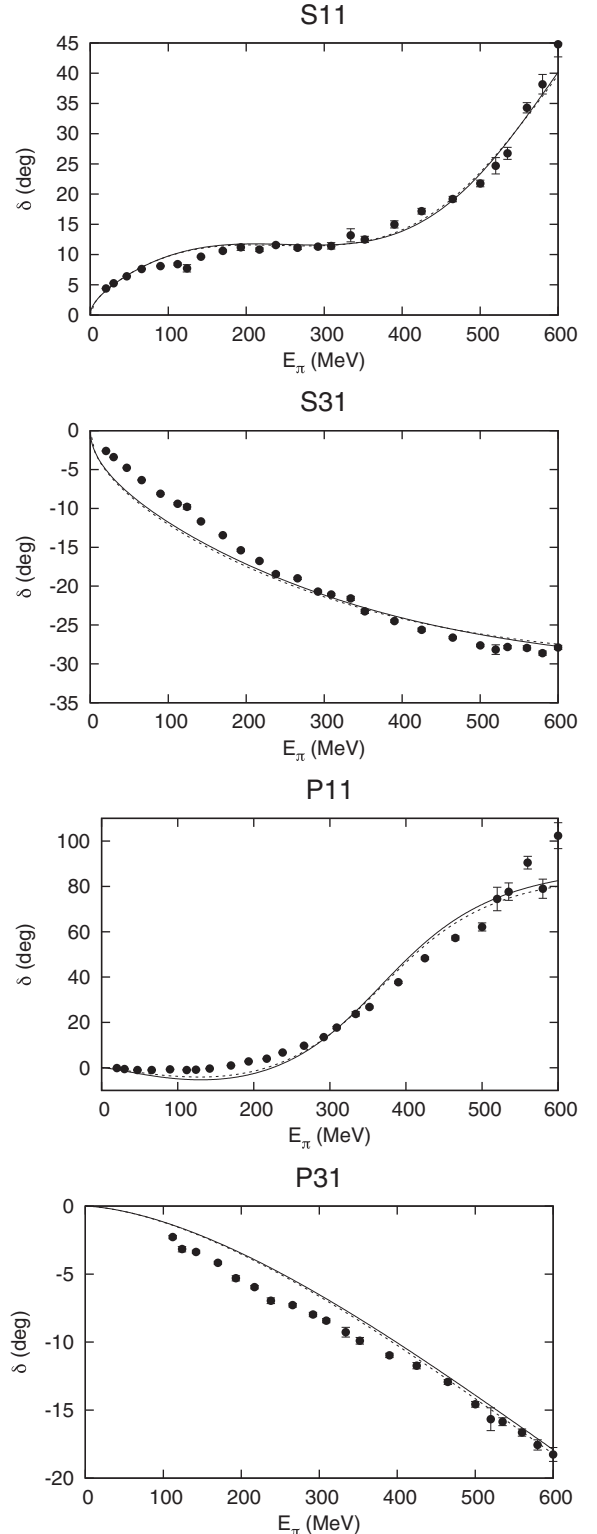

FIG. 4. Phase shifts for $j = 1/2$. Fit A results (dotted lines) are almost indistinguishable from those for Fit B (solid lines). The data are taken from [28].

$p^2 = (m_N + m_\pi)^2 - i\epsilon$ to $p^2 = \infty - i\epsilon$ when $|\mathbf{r}|$ is integrated from 0 to ∞. This cut can be moved across m_R^2 by rotating the $|\mathbf{r}|$ integral using the replacement $|\mathbf{r}| \to |\mathbf{r}| e^{-i\phi}$, with

TABLE II. Parameters that are determined by the fits. The masses m_{N0}, m_{R0}, M_R are in units of MeV and the other parameters are dimensionless.

	A	B
$\sqrt{Z_N}$	1.09671	0.91862
$\sqrt{Z_R}$	0.04759	0.04069
$\sqrt{Z_2}$	1.04774	0.96018
m_{N0}	1032.45740	1047.36929
m_{R0}	1967.19681	1832.62105
M_R	$1362.9 - 96.8i$	$1362.7 - 96.7i$
$g_{\pi NN}$	12.79023	12.97247

$\phi \gtrsim 12.5$ degrees. The squared Roper mass then ends up on the second sheet of the p^2 Riemann surface, as required.

We have restricted m_{R0} to being real in order to preserve unitarity. This condition made giving g^+ a pole exactly at the Roper mass rather difficult, and the Fit A parameters cause it to have a pole at $M_R = 1362.9 - 96.8i$ MeV, which is slightly different from m_R.

Another issue with Fit A is the fact that Z_2, which is interpreted as being a probability, is greater than 1 (see Table II). In exact field theory, the only singularities that $g_N^+(p_0)$ contributes to the p_0 plane are a pair of cuts running from $\pm(m_N + m_\pi - i\epsilon)$ to $\pm(\infty - i\epsilon)$, and it can be shown that this results in Z_2 being restricted to the range $0 \leqslant Z_2 \leqslant 1$. Introducing cutoff factors such as h_α, however, gives $g_N^+(p_0)$ extra poles, and this allows Z_2 to move outside the unitary bound. The spectator approach also modifies the structure: when replacement (51) is used inside $g_N^+(p_0)$, the cuts move so that they run from $p_0 = 0 + i\epsilon$ to $p_0 = m_N - m_\pi + i\epsilon$ and from $p_0 = m_N + m_\pi - i\epsilon$ to $p_0 = \infty - i\epsilon$ instead. We found it impossible to obtain both a decent fit to the phase shifts and a Z_2 in the correct range when replacement (51) was used.

It turns out, however, that if the spectator approach is implemented by putting both nucleons and antipions on shell, the correct cut structure can be preserved. Thus, we also tried using the two-term spectator approach,

$$G_0(k', r', k, r) \rightarrow (2\pi)^4 \delta^4(k' - k) Z_2 \frac{\pi i (\not{r} + m_N)}{p_0 - E_r + \omega_k}$$

$$\times \left[\frac{\delta^+(r^2 - m_N^2)}{E_r(p_0 - \omega_k - E_r + i\epsilon)} + \frac{\delta^-(k^2 - m_\pi^2)}{\omega_k(p_0 + \omega_k + E_r - i\epsilon)} \right] \quad (59)$$

where $\omega_k = \sqrt{\mathbf{k}^2 + m_\pi^2}$. The first and second terms in the large square brackets put nucleons and antipions on shell and, together, contribute cuts to the p_0 plane that are the same as those in full four-dimensional field theory. The denominator outside the square brackets does not contribute any cut structure because when it passes through zero the square bracketed terms cancel. It should be noted, however, that the prescription of Eq. (59) does not follow from the type of analysis that led GS to set the pion on mass shell in their model [25].

A set of parameters corresponding to replacement (59) is labeled as Fit B in Tables I and II. The phase shifts for this fit are almost indistinguishable from the Fit A results, and Z_2 falls in the correct range despite the poles contributed by the cutoff factors.

V. GAUGING THE STRONG INTERACTION MODEL

In this section, expressions for the gauged bare πNN vertices, gauged potential, and gauged intermediate propagators are presented. They are needed as input to the pion-photon vertex and pion photoproduction amplitude given in Sec. III.

A. Gauged bare πNN vertex

To gauge the bare πNN vertices, we use the method of minimal substitution. The application of this procedure to πNN vertices with cutoff factors is discussed at length in the Ph.D. thesis of van Antwerpen [29] (an abridged version of which was published in [30]). By taking a combination of his results for pseudoscalar and pseudovector coupling, we can immediately write

$$f_{\alpha 0}^{\mu a}(k', r', r) = \Pi_{k'}^{\mu ab} \left[f_{\alpha 0}^b(k', r', r) - f_{\alpha 0}^b(k' - q, r', r) \right]$$

$$+ \left[f_{\alpha 0}^a(k', r', r + q) - f_{\alpha 0}^a(k', r', r) \right] \Pi_r^\mu$$

$$+ \Pi_{r'}^\mu \left[f_{\alpha 0}^a(k', r', r) - f_{\alpha 0}^a(k', r' - q, r) \right]$$

$$- \gamma_5 Z_2^{-1/2} F_V[(k' - q)^2, r'^2] h_\alpha(r'^2) g_{\pi N\alpha}^{(0)} y_\alpha$$

$$\times \left(i\gamma^\mu \lambda_{\pi ab} + \Pi_{k'}^{\mu ab} \not{q} \right) \tau_b^*, \quad (60)$$

where

$$\Pi_{k'}^{\mu ab} = i\lambda_{\pi ab} \frac{2k'^\mu - q^\mu}{(k' - q)^2 - k'^2},$$

$$\Pi_r^\mu = i\lambda_N \frac{2r^\mu + q^\mu}{r^2 - (r + q)^2},$$

$$\Pi_{r'}^\mu = i\lambda_N \frac{2r'^\mu - q^\mu}{(r' - q)^2 - r'^2}. \quad (61)$$

It is easy to verify that this gauged vertex satisfies identity (25). The $f_{\alpha 0}^a(k', r', r)$ terms on the RHS of Eq. (60) do not contribute to the WTI, but play an important role in ensuring that $f_{\alpha 0}^\mu$ does not contain any poles. Whenever the denominators in the Π factors pass through zero, these terms cause the numerators to vanish and give a derivative.

Similarly, the gauged pion absorption vertex is given by

$$\bar{f}_{\alpha 0}^{\mu a}(k, r', r) = \left[\bar{f}_{\alpha 0}^b(k + q, r', r) - \bar{f}_{\alpha 0}^b(k, r', r) \right] \Pi_k^{\mu ba}$$

$$+ \left[\bar{f}_{\alpha 0}^a(k, r', r + q) - \bar{f}_{\alpha 0}^a(k, r', r) \right] \Pi_r^\mu$$

$$+ \Pi_{r'}^\mu \left[\bar{f}_{\alpha 0}^a(k, r', r) - \bar{f}_{\alpha 0}^a(k, r' - q, r) \right]$$

$$- \tau_b Z_2^{-1/2} g_{\pi N\alpha}^{(0)} F_V[(k + q)^2, r^2] h_\alpha(r'^2) y_\alpha$$

$$\times \left(i\gamma^\mu \lambda_{\pi ba} + \Pi_k^{\mu ba} \not{q} \right) \gamma_5, \quad (62)$$

where

$$\Pi_k^{\mu ba} = i\frac{2k^\mu + q^\mu}{k^2 - (k+q)^2}\lambda_{\pi ba}. \tag{63}$$

B. Gauged potential

To gauge the background potential v, we begin by using the product rule on the first of Eqs. (56):

$$v_{ba}^\mu(k', r'+q, k, r) = F_L^{\mu bat}\tilde{v}_t(p)F_R + F_{Lp}\tilde{v}_t^{\mu ba}(p+q, p)F_R$$
$$+ F_{Lp}\tilde{v}_t(p+q)F_R^{\mu bat}, \tag{64}$$

where $p = k + r = k' + r'$ and $\tilde{v}_t = -iZ_2^{-1}\tilde{\mathcal{V}}_t$. F_{Lp} and F_R are products of cutoff factors with the momentum dependences

$$F_{Lp} = F_V[k'^2, (r'+q)^2], \quad F_R = F_V(k^2, r^2). \tag{65}$$

To gauge the functions of momentum we again borrow from van Antwerpen's results and use

$$F_L^{\mu bat} = \left[(F_L - F_{Lk'})\Pi_{k'}^{\mu bn} + (F_L - F_{Lr'})\Pi_{r'}^\mu \delta_{bn}\right](P_t)_{na}$$
$$+ (F_{Lp} - F_L)\Pi_p^{\mu bat},$$

$$F_R^{\mu bat} = (P_t)_{bn}\left[(F_{Rk}-F_{Rp})\Pi_k^{\mu na} + (F_{Rr}-F_{Rp})\Pi_r^\mu \delta_{na}\right]$$
$$+ (F_{Rp} - F_R)\Pi_p^{\mu bat},$$

$$\tilde{v}_t^{\mu ba}(p+q, p) = [\tilde{v}_t(p+q) - \tilde{v}_t(p)]\Pi_p^{\mu bat}$$
$$+ iZ_2^{-1}\lambda_T^{bat}C_0^t([p+q]^2)$$
$$\times \left[\gamma^\mu - \frac{q\!\!\!/(2p^\mu + q^\mu)}{(p+q)^2 - p^2}\right], \tag{66}$$

where

$$F_L = F_V[k'^2, (r'+q)^2], \qquad F_{Rp} = F_V(k^2, r^2),$$
$$F_{Lk'} = F_V[(k'-q)^2, (r'+q)^2], \quad F_{Rk} = F_V[(k+q)^2, r^2],$$
$$F_{Lr'} = F_V(k'^2, r'^2), \qquad F_{Rr} = F_V[k^2, (r+q)^2], \tag{67}$$

and

$$\Pi_p^{\mu bat} = \frac{2p^\mu + q^\mu}{p^2 - (p+q)^2}\lambda_T^{bat}. \tag{68}$$

Since p is the total momentum of the pion-nucleon system it has been associated with the total "charge":

$$\lambda_T^{bat} = i(\lambda_N\delta_{bn} + \lambda_{\pi bn})(P_t)_{na} = i(P_t)_{bn}(\lambda_N\delta_{na} + \lambda_{\pi na}). \tag{69}$$

Putting the pieces together, a gauged potential that satisfies WTI (12) is obtained. The C functions in this v^μ depend only on p and q and do not participate in any integrals, resulting in v^μ retaining the separability of the original potential.

C. Gauging on-shell particles

When the spectator approach is implemented by putting intermediate nucleons on shell, there are two possible ways of applying it to diagrams that have two internal nucleon lines within a single loop, such as the fifth diagram on the RHS of Fig. 2. In order to satisfy the WTI, Gross, and Riska [31] approximated diagrams such as this by replacing them with two terms. In one term, the particle to the left of the photon vertex was put on shell, and in the other the particle to the right of the photon vertex received the same treatment. However, because this prescription leads to the nonconservation of charge, we will use a modified version suggested by [13]:

$$G_0^\mu(k', r', k, r) \rightarrow G_N^\mu(k', r', k, r) + G_\pi^\mu(k', r', k, r), \tag{70}$$

where we now have $k' + r' = k + r + q = p + q$ and

$$G_N^\mu(k', r', k, r) = -Z_2(2\pi)^4\delta^4(k' - k)(r\!\!\!/' + m_N)\Gamma_{N0}^\mu(r', r)(r\!\!\!/ + m_N)$$

$$\times \left[\frac{\pi}{E_{r'}} \frac{\delta^+(r'^2 - m_N^2)}{(E_r + q_0 - E_{r'})(q_0 - E_{r'} - E_r)(p_0 + q_0 - E_{r'} - \omega_k + i\epsilon)(p_0 + q_0 - E_{r'} + \omega_k - iz\epsilon)}\right.$$

$$+ \frac{\pi}{E_r} \frac{\delta^+(r^2 - m_N^2)}{(E_r + q_0 - E_{r'})(E_r + q_0 + E_{r'})(p_0 - E_r - \omega_k + i\epsilon)(p_0 - E_r + \omega_k - iz\epsilon)}$$

$$\left.+ \frac{\pi}{\omega_k} \frac{\delta^-(k^2 - m_\pi^2)(1 - z)}{(p_0 + \omega_k - E_r)(p_0 + \omega_k + E_r - i\epsilon)(p_0 + q_0 + \omega_k - E_{r'})(p_0 + q_0 + \omega_k + E_{r'} - i\epsilon)}\right], \tag{71a}$$

$$G_\pi^\mu(k', r', k, r) = -Z_2(2\pi)^4\delta^4(r' - r)(r\!\!\!/ + m_N)\Gamma_\pi^\mu(k', k)$$

$$\times \left[\frac{\pi}{\omega_{k'}} \frac{\delta^-(k'^2 - m_\pi^2)(1 - z)}{(q_0 + \omega_{k'} - \omega_k)(q_0 + \omega_{k'} + \omega_k)(p_0 + q_0 + \omega_{k'} - E_r)(p_0 + q_0 + \omega_{k'} + E_r - i\epsilon)}\right.$$

$$+ \frac{\pi}{\omega_k} \frac{\delta^-\left(k^2 - m_\pi^2\right)(1 - z)}{(q_0 - \omega_k - \omega_{k'})(q_0 - \omega_k + \omega_{k'})(p_0 + \omega_k - E_r)(p_0 + \omega_k + E_r - i\epsilon)}$$

$$+ \frac{\pi}{E_r} \frac{\delta^+\left(r^2 - m_N^2\right)}{(p_0 + q_0 - E_r - \omega_{k'} + i\epsilon)(p_0 + q_0 - E_r + \omega_{k'} - iz\epsilon)(p_0 - E_r - \omega_k + i\epsilon)(p_0 - E_r + \omega_k - iz\epsilon)} \Bigg].$$

$$(71b)$$

If prescription (51) is used to implement the spectator approach in G_0, $z = 1$ should be chosen; $z = 0$ corresponds to prescription (59).

In G_N^μ the delta function demands $k' = k$ and hence $r = p - k$, $r' = p + q - k$. Meanwhile, G_π^μ has $r' = r$ and hence $r = p - k$, $k' = k + q$. With that in mind, it is easy to see that G_N^μ and G_π^μ remain regular when the square bracketed denominators without $i\epsilon$ terms go to zero. For instance, when $q_0 = \omega_k - \omega_{k+q}$, we have $\omega_{k+q} + \omega_k + q_0 = 2\omega_k$, $q_0 - \omega_k - \omega_{k+q} = -2\omega_{k+q}$, and $p_0 + q_0 + \omega_{k+q} = p_0 + \omega_k$. The first two terms contained in the large curly brackets of Eq. (71b) therefore cancel out and result in a derivative rather than a singularity.

Note that the denominators in the round brackets cannot pass through zero when $q^2 \leqslant 0$ (this is the only case that we will be considering). When $-|\mathbf{q}| \leqslant q_0 \leqslant 0$ it is obviously impossible to have $\omega_{k+q} + \omega_k - q_0 = 0$. If we also have a case of $|\mathbf{q}| < |\mathbf{k}|$ then

$$-\omega_{k+q} - \omega_k < -|\mathbf{k}| < -|\mathbf{q}| \leqslant q_0 \qquad (72)$$

and it is not possible for $\omega_k + \omega_{k+q} + q_0$ to pass through zero either. Now consider the situation of $|\mathbf{q}| \geqslant |\mathbf{k}|$. In the extreme case where $\mathbf{q}$ is parallel to $\mathbf{k}$ we have

$$-\omega_{k+q} - \omega_k = -\sqrt{(|\mathbf{k}| + |\mathbf{q}|)^2 + m_\pi^2} - \sqrt{\mathbf{k}^2 + m_\pi^2}$$
$$< -|\mathbf{q}| \leqslant q_0. \qquad (73)$$

In the other extreme case where $\mathbf{k}$ is antiparallel to $\mathbf{q}$ we have

$$-\omega_{k+q} - \omega_k = -\sqrt{(|\mathbf{k}| - |\mathbf{q}|)^2 + m_\pi^2} - \sqrt{\mathbf{k}^2 + m_\pi^2}$$
$$< -|\,|\mathbf{k}| - |\mathbf{q}|\,| - |\mathbf{k}|$$
$$\leqslant q_0 \qquad (74)$$

Thus the zeros of all round bracketed denominators are excluded. A proof that is nearly identical to the one above shows that the zeros of $\pm(\omega_{k+q} + \omega_k) - q_0$ are inaccessible for $0 \leqslant q_0 \leqslant |\mathbf{q}|$ as well.

VI. NUCLEON ELECTROMAGNETIC FORM FACTORS

We now have the ingredients to calculate the photon-nucleon vertex in Eq. (45). To test its accuracy, nucleon electromagnetic form factors have been extracted. This is done by using Lorentz invariance and the Gordon identity to express the on-shell version of Γ_Z^μ as,

$$\bar{u}(\mathbf{p}')\Gamma_Z^\mu(p', p)u(\mathbf{p})$$
$$= e\bar{u}(\mathbf{p}')\left[F_1(q^2)\gamma^\mu + \frac{i\sigma^{\mu\nu}q_\nu}{2m_N}F_2(q^2)\right]u(\mathbf{p}), \qquad (75)$$

where it is assumed that $p^2 = p'^2 = m_N^2$. The Dirac matrix coefficients F_1, F_2 are the electromagnetic form factors and are 2×2 matrices in isospin space. They can be decomposed into proton and neutron components:

$$F_{1,2} = \frac{1 + \tau_3}{2}F_{1,2}^p + \frac{1 - \tau_3}{2}F_{1,2}^n. \qquad (76)$$

It is conventional to report the form factors in the combinations

$$G_E(q^2) = F_1(q^2) + \frac{q^2}{4m_N^2}F_2(q^2),$$
$$G_M(q^2) = F_1(q^2) + F_2(q^2), \qquad (77)$$

which are the Sachs form factors. Those obtained from the Fit A parameters and prescription (51) are shown in Fig. 5, denoted by the dot-dot-dashed lines. The G_E^p and G_M^p data are taken from [32], the G_E^n data from [33,34], and the G_M^n data from [35,36]. That we have obtained $G_E^p(0) = 1$, $G_E^n(0) = 0$ is a strong indication that the Ward identity is satisfied and that gauge invariance is being maintained. The curve for G_M^n also predicts the data with reasonable accuracy. However, the G_E curves have slopes with signs opposite to what they should be, while that for G_M^p has a magnitude that is too large. The wrong slope of G_E^p at $q^2 = 0$ is particularly significant as it implies a negative mean square charge radius $\langle r^2 \rangle$ for the proton [37], a result that seems to be connected to the problem of $Z_2 > 1$ for the Fit A case.

The Fit B form factors are denoted by the dot-dashed lines in Fig. 5. The slopes of these curves all have the correct signs, but they are not steep enough and the magnitudes of $G_M^{n,p}(0)$ are not very good either.

Overall, it would appear that our model, as it stands, is incapable of describing the EM form factors for $q^2 < 0$. There are, on the other hand, a lot of successful models in the literature. One early theory postulated that photons, after turning into quark-antiquark pairs, couple to nucleons as vector mesons. The vector meson propagators have a dipole form, and when enough exchange diagrams are included in these vector meson dominance models, they are able to fit the form factor data very well without including any pion loops at all [38,39]. However, these models are essentially phenomenological, and impart little information about the underlying nucleon structure. Other early calculations were based
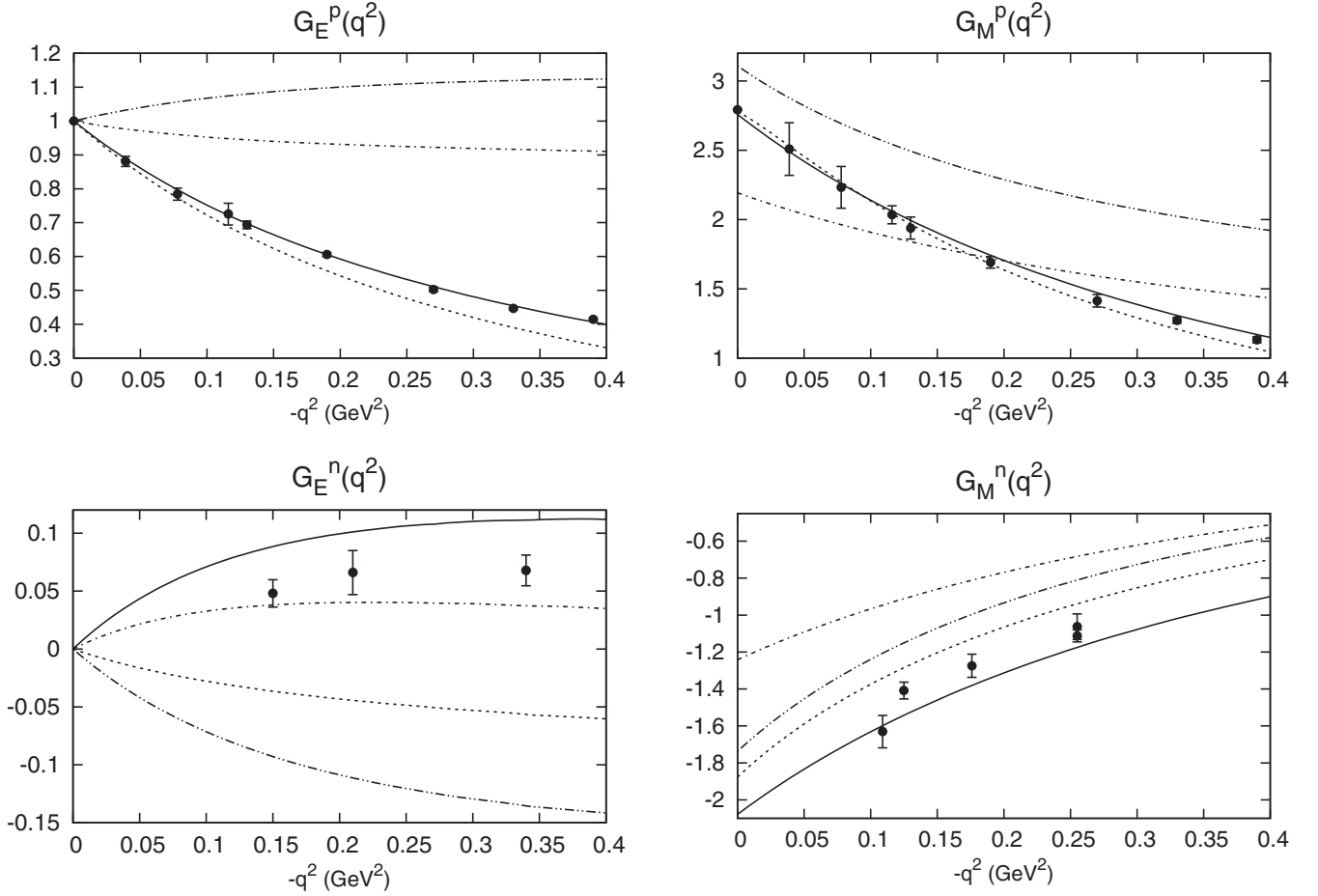
FIG. 5. Nucleon electromagnetic form factors. The meaning of the different line types is explained in the text.

on dispersion theory [40,41]. More recently, nucleon form factor calculations have used lattice QCD [42,43], cloudy bag models [44], quark models [45,46], and chiral perturbation theory [47–49]. The latter calculations involve pion loop diagrams, but are based on quite complicated Lagrangians. Accordingly, the bare γNN vertices have a lot of physics in them. In contrast, we have simply used $\frac{e}{2}(1 + \tau_3)\gamma^\mu$ for this vertex. That this choice for the vertex is inadequate is further evidenced by the poor results at large $-q^2$ where all loop diagrams in Fig. 1 are expected to vanish, thus leaving only $Z_2\Gamma_{N0}^\mu$ to describe the data. Another possible source of error is that, having removed the dressing from the two-particle intermediate states, all γNN vertices appearing inside our pion loops are bare ones. This has resulted in Γ_N^μ being the solution of an ordinary equation rather than an integral one. However, since Γ_Z^μ still contains an infinite number of diagrams we will assume an inadequate choice of bare γNN vertex is the main reason our calculations give such poor results.

Accordingly, we replaced all instances of Γ_{N0}^μ with

$$\Gamma_{N0}^\mu \rightarrow \tilde{F}_1(q^2)\gamma^\mu + \tilde{F}_2(q^2)\frac{i}{2m_N}\sigma^{\mu\nu}q_\nu + \tilde{F}_3(q^2)\,\slashed{q}q^\mu \quad (78)$$

The first two coefficients are chosen to have the dipole form

$$\tilde{F}_1(q^2) = e\frac{1}{(1 - b_1 q^2)^2}\frac{1 + \tau_3}{2},$$

$$\tilde{F}_2(q^2) = e\frac{a_{2p}}{(1 - b_{2p}q^2)^2}\frac{1 + \tau_3}{2} + e\frac{a_{2n}}{(1 - b_{2n}q^2)^2}\frac{1 - \tau_3}{2}. \quad (79)$$

The remaining coefficient in Eq. (78), which is included so that the new Γ_{N0}^μ satisfies the WTI, is

$$\tilde{F}_3(q^2) = \frac{1}{q^2}\left[e\frac{1 + \tau_3}{2} - \tilde{F}_1(q^2)\right]. \quad (80)$$

Since $\tilde{F}_1(0) = \frac{e}{2}(1 + \tau_3)$, $\tilde{F}_3(q^2)$ in the limit $q^2 \rightarrow 0$ is a finite quantity involving the derivative of $\tilde{F}_1$ with respect to q^2. With this new bare vertex, the calculation is able to achieve a good description of the data, as shown by the dashed (Fit A) and solid (Fit B) lines in Fig. 5. The parameters b_1, $b_{2\alpha}$, and $a_{2\alpha}$ are given in Table III.

Overall, the results of Fig. 5 provide an explicit example of how the assumption of a "bare" nucleon is in contradiction with the experimental data, and that the nucleon should be considered as a composite particle.

TABLE III. Parameters of the bare γNN vertex in Eq. (78). The b parameters have units of GeV^{-2}, while the a's are dimensionless.

	A	B
b_1	2.000	1.408
b_{2p}	10.000	1.408
b_{2n}	1.111	1.408
a_{2p}	−0.260	0.715
a_{2n}	−0.100	−0.978

FIG. 6. Terms that contribute to $\gamma N \to \pi N$ but which are not included in our model.

VII. MULTIPOLE AMPLITUDES

We now come to calculating the $\gamma N \to \pi N$ amplitude of Eq. (50). All the parameters have already been set either by the πN phase shifts or by the EM form factors and there is no further adjustment. The results presented in this section are therefore all predictions of the data, rather than fits to it.

It is convenient to work in the center of mass of the incoming photon and nucleon, and for the motion of the final state pion and nucleon to be in the xz plane. This corresponds to the kinematics $T_Z^{\mu a}(k_f, p - k_f, p_i)$, where

$$k_f = (\omega_{\bar{k}}, \bar{k}\sin\theta, 0, \bar{k}\cos\theta), \quad p_i = (E, 0, 0, -\bar{q}),$$

$$q = (\bar{q}, 0, 0, \bar{q}), \qquad E = \sqrt{\bar{q}^2 + m_N^2},$$

$$\bar{q} = \frac{p_0^2 - m_N^2}{2p_0}, \qquad p_0^2 = 2E_\gamma m_N + m_N^2. \quad (81)$$

The momenta of the incoming nucleon, outgoing pion, and the photon are denoted by p_i, k_f, and q, respectively. They are all taken to be on shell. The total momentum of the $\pi N\gamma$ system is $p = p_i + q$ and, since we require $p_0 > m_N + m_\pi$ to produce a pion, the energy of the incoming photon E_γ must be chosen to be greater than $m_\pi + m_\pi^2/(2m_N) \approx 148$ MeV. The on-shell relative momentum is given by

$$\bar{k} = \sqrt{\frac{[p_0^2 - (m_N + m_\pi)^2][p_0^2 - (m_N - m_\pi)^2]}{4p_0^2}}. \quad (82)$$

In calculating $T_Z^{\mu a}$, the dressed propagator and photon vertex in the crossed Born term $\boldsymbol{v}_u^{\mu a}$ have been replaced by their bare equivalents. That is to say we have made the replacement

$$\boldsymbol{v}_u^{\mu a}(k', r', r) \to \Gamma_{N0}^\mu \frac{i}{\not{r}' - \not{q} - m_N + i\epsilon} \boldsymbol{f}^a(k', r' - q, r). \quad (83)$$

The resulting $T_Z^{\mu a}$ is the same as the one obtained by attaching photons in all possible ways to $\tilde{g}_{N0}g_\pi \boldsymbol{fg}$, where $\tilde{g}_{N0}$ is the same as g_{N0} but for a particle of mass m_N. We tried calculating the $\boldsymbol{v}_u^\mu$ of Eq. (49b) by boosting the dressed propagator and vertices to moving frames, but did not obtain very good results. This is understandable, though, because the parameters have been set for the specific case of the dressed quantities being in stationary frames.

We have also left out the Δ resonance and heavy meson exchange diagrams of Figs. 3 and 6, even though they are needed
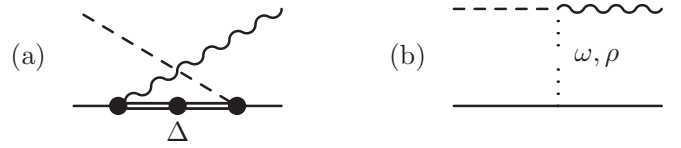
to describe certain photoproduction data. The Δ diagrams, for instance, have a large impact on a number of multipole amplitudes, particularly those for which the total isospin t or total angular momentum j are equal to 3/2. However, the exact size of their contribution is in part determined by the Δ electromagnetic form factors, and because these are not well known they are usually taken to be free parameters (as in, for example, [3,5,6]). As we are primarily concerned with studying the ability of $T_Z^{\mu a}$ to predict, rather than simply describe, the data, we have dropped the Δ diagrams and concentrated on the amplitudes for which $j = 1/2$, $t = 1/2$. The Δ is not expected to contribute much (if at all) to these channels.

Likewise, the meson exchange diagrams are neglected because they can also be expected to make a fairly small contribution to the $j = 1/2$, $t = 1/2$ amplitudes (compare the dotted and dash-dotted curves in Figs. 3 and 4 of Ref. [6] for an example of this).

The multipole amplitudes were extracted from $T_Z^{\mu a}$ using the formulas written in Appendix C 2. These amplitudes are labeled with the notation $M_{l\pm}(t)$ and $E_{l\pm}(t)$, where l is the orbital angular momentum of the emitted pion and the $\pm$ sign indicates the total angular momentum $j = l \pm \frac{1}{2}$. M denotes magnetic multipole amplitudes and E the electric ones; using Eq. (C13) these are further decomposed into proton and neutron components which are labeled by subscript n's and p's.

The $j = 1/2$, $t = 1/2$ proton multipole amplitudes are shown in Fig. 7, where the different line styles denote the same scenarios as in Fig. 5. The neutron amplitudes, shown in Fig. 8, are of similar quality. When $\Gamma_{N0}^\mu = \frac{1}{2}e(1 + \tau_3)\gamma^\mu$ is used, the curves for Fit A are mostly quite close to the data, although those for $M_{1-}(1/2)$ have magnitudes that are a little too large. Parametrizing the photon-nucleon vertices according to Eq. (78) makes no appreciable difference to the $E_{0+}(1/2)$ amplitudes, but causes the $M_{1-}(1/2)$ ones to become less accurate in the case of Fit A. A possible explanation for this is that since the parametrization has been set up to correct the on-shell version of Γ^μ, the γNN vertices appearing in diagrams other than the uncrossed Born term $\boldsymbol{v}_s^{\mu a}$ do not have the right on-shell values (the γNN vertices in diagrams other than $\boldsymbol{v}_s^{\mu a}$ are just Γ_{N0}^μ). It is also possible that, in addition to making the on-shell form factors more accurate, the parametrization has the side effect of making the off-shell vertices less so.

The $M_{1-}(1/2)$ curves for Fit B, on the other hand, show an improvement when the bare photon vertex is parametrized. Using $\frac{1}{2}e(1 + \tau_3)\gamma^\mu$ for Γ_{N0}^μ produces curves that are not too bad, although their magnitudes are a little too large at
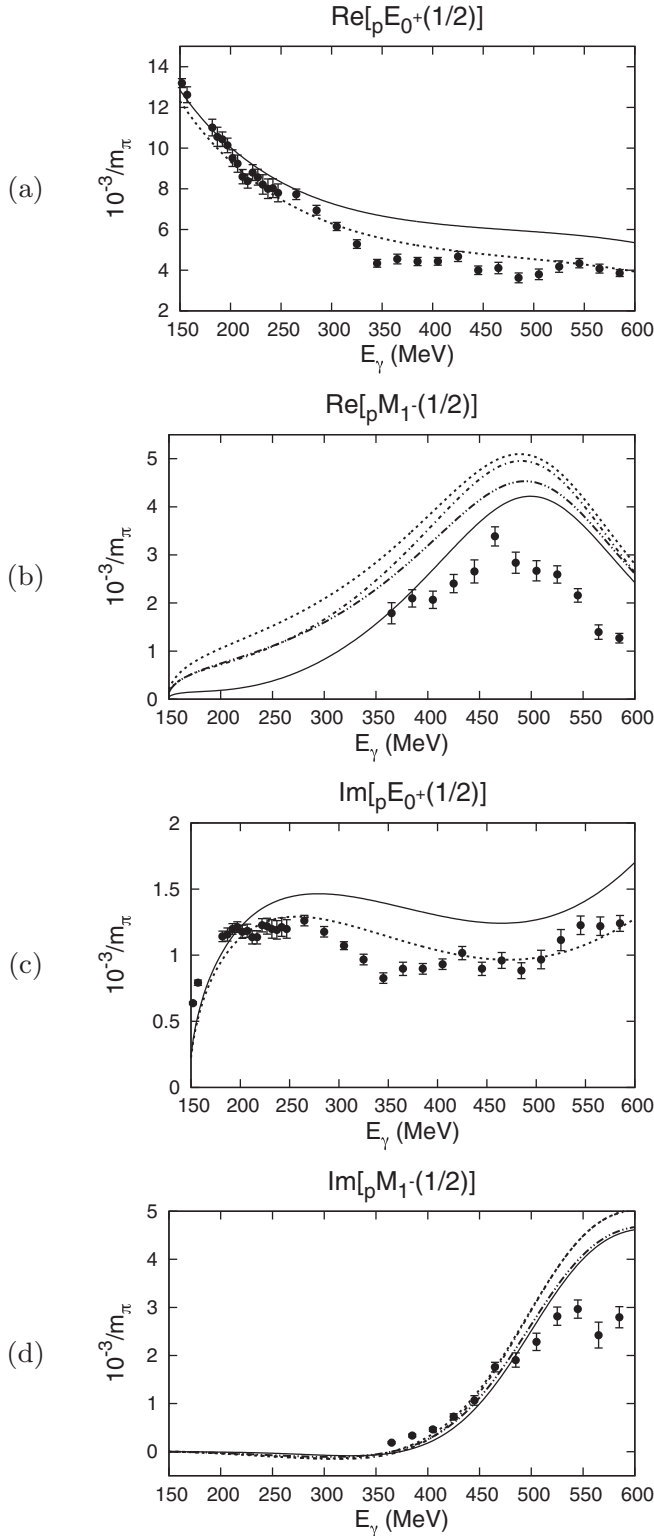
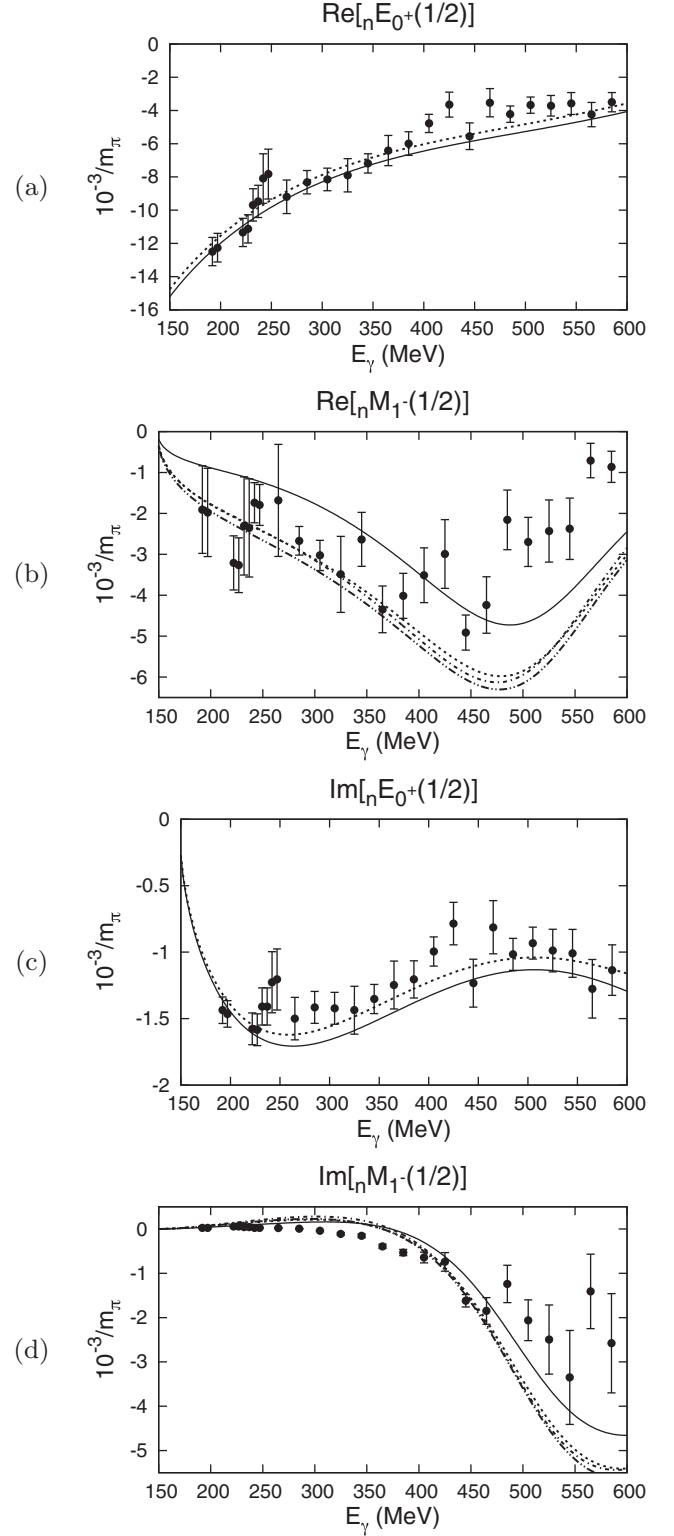FIG. 7. Proton multipole amplitudes for $j = 1/2$, $t = 1/2$. The various line styles denote the same cases as in Fig. 5, while the data are taken from [28].

FIG. 8. Neutron multipole amplitudes for $j = 1/2$, $t = 1/2$. The various line styles denote the same cases as in Fig. 5.

energies greater than about 300 MeV. Parametrizing Γ_{N0}^μ, however, moves the M_{1-} curves downward and makes them more accurate.

VIII. CONCLUSION

In this paper we have calculated a $\gamma N \to \pi N$ amplitude that has both unitarity and gauge invariance. For the first time,

gauge invariance has been achieved through the complete attachment of photons to an infinite set of $N \to \pi N$ diagrams.

In these covariant initial investigations, we have chosen to reduce loop integrals to three dimensions using the covariant spectator approach. The results obtained so far are encouraging: there have been no insurmountable technical difficulties and the $\gamma N \to \pi N$ amplitudes predict photoproduction data for $j = 1/2$, $t = 1/2$ fairly well (these are the channels to which only diagrams involving pions and nucleons are expected to make significant contributions). The model can be easily extended to describe amplitudes for $j > 1/2$, $t > 1/2$ through the addition of extra nucleon resonances and heavy meson exchange diagrams.

Meanwhile, the dressed photon-baryon vertex Γ^μ that is an input to the $\gamma N \to \pi N$ calculation gives a reasonable prediction of the nucleon electromagnetic form factors for on-shell ($q^2 = 0$) photons. To get a good description of the form factors for $q^2 < 0$, we found it necessary to parametrize the bare photon-nucleon vertex. Happily, this parametrization also improved the quality of the Fit B $M_{1-}(1/2)$ multipole amplitudes.

The numerical calculations we have presented in this paper successfully illustrate how the gauging of equations method can be used in practice, and it is hoped that the results will be useful for future developments.

ACKNOWLEDGMENTS

APPENDIX A: Nucleon and Roper propagators

1. Nucleon propagator

In order to determine bare masses and coupling constants in our description, it is useful to decompose the nucleon propagator into positive and negative energy components, as illustrated by the well-known covariant identity for the bare nucleon propagator:

$$\frac{1}{\not{p} - m + i\epsilon} = \frac{m}{E}\left[\frac{\Lambda^+(\mathbf{p})}{p_0 - E + i\epsilon} - \frac{\Lambda^-(-\mathbf{p})}{p_0 + E - i\epsilon}\right]. \quad (A1)$$

In this expression $E = \sqrt{\mathbf{p}^2 + m^2}$, and $\Lambda^\pm(\mathbf{p})$ are the positive and negative energy projection operators given by

$$\Lambda^\pm(\mathbf{p}) = \frac{m \pm \bar{\not{p}}}{2m} \quad \text{where } \bar{p} = (E, \mathbf{p}). \quad (A2)$$

For the dressed nucleon propagator, an analogous decomposition can be made, but it takes on a more complicated form [50]:

$$-ig_N(p) = g^+(p)\Lambda^+(\mathbf{p}) + g_1^-(p)\Lambda^-(-\mathbf{p}) + g_2^-(p)\Lambda^-(\mathbf{p}). \quad (A3)$$

In order to simplify the algebra, we work in the center-of-mass (c.m.) system where $p = (p_0, \mathbf{0}) \equiv (\sqrt{s}, \mathbf{0})$, in which case Eq. (A3) reduces to a form similar to that of Eq. (A1):

$$-ig_N(p) = g^+(p_0)\Lambda^+ + g^+(p_0)\Lambda^-, \quad (A4)$$

where $\Lambda^\pm \equiv \Lambda^\pm(\mathbf{0}) = (1 \pm \gamma_0)/2$. Expressed in this way, the pole and residue (Z_2) of $g_N(p)$ at $\not{p} = m_N$, where m_N is the dressed nucleon mass, is manifest as the pole and residue of the positive energy component $g^+(p_0)$ at $p_0 = m_N$. In order to show this explicitly, we first consider the dressed nucleon propagator in its covariant form

$$-ig_N(p) = \frac{1}{\not{p} - m_{N0} - \tilde{\Sigma}_N(p) + i\epsilon}, \quad (A5)$$

where the dressing term $\tilde{\Sigma}_N(p) = i\Sigma_N(p)$ is expressed in its most general form as

$$\tilde{\Sigma}_N(p) = \not{p}A(p^2) + m_N B(p^2) \quad (A6)$$

with $A(p^2)$ and $B(p^2)$ being scalar functions. Then the requirement that $g_N(p)$ have a pole at $\not{p} = m_N$ leads to the expressions

$$m_{N0} = m_N\left[1 - A\left(m_N^2\right) - B\left(m_N^2\right)\right] \quad (A7)$$

for the bare mass and

$$Z_2 = \left.\frac{1}{A(s) - 2m_N^2[A'(s) + B'(s)]}\right|_{s=m_N^2} \quad (A8)$$

for the residue of $g_N(p)$ at the $\not{p} = m_N$ pole. By then considering Eq. (A5) specifically in the c.m., one finds the following expressions for the positive and negative energy components appearing in Eq. (A4):

$$g_N^+(p_0) = \frac{1}{[1 - A(s)]p_0 - m_0 - mB(s) + i\epsilon}, \quad (A9a)$$

$$g_N^-(p_0) = \frac{1}{[A(s) - 1]p_0 - m_0 - mB(s) + i\epsilon}, \quad (A9b)$$

where $s = p_0^2$. It can then be checked explicitly that $g_N^+(p_0)$ has a pole at $p_0 = m_N$ with residue Z_2.

2. Nucleon propagator with Roper mixing

The nucleon (N) and the Roper resonance (R) have the same quantum numbers and therefore can couple via self-interactions. Denoting the one-particle irreducible amplitudes for transitions $N \to N, R \to N, N \to R$, and $R \to R$, by Σ_{NN}, Σ_{NR}, Σ_{RN}, and Σ_{RR}, respectively, it is useful to first define propagators g_N and g_R through the equations

$$g_N^{-1} = g_{N0}^{-1} - \Sigma_{NN}, \quad (A10a)$$

$$g_R^{-1} = g_{R0}^{-1} - \Sigma_{RR}. \quad (A10b)$$

These, however, are not the physical nucleon and Roper dressed propagators as they contain no nucleon-Roper couplings. Instead, we denote the propagators with full nucleon-Roper coupling by $g_{NN}, g_{NR}, g_{RN}, g_{RR}$, and these are most easily described by defining the matrices

$$\mathbf{g} = \begin{pmatrix} g_{NN} & g_{NR} \\ g_{RN} & g_{RR} \end{pmatrix}, \quad \mathbf{g}_0 = \begin{pmatrix} g_{0N} & 0 \\ 0 & g_{0R} \end{pmatrix}, \quad (A11)$$

$$\mathbf{\Sigma} = \begin{pmatrix} \Sigma_{NN} & \Sigma_{NR} \\ \Sigma_{RN} & \Sigma_{RR} \end{pmatrix}. \quad (A12)$$

One can then write a set of coupled equations for these propagators as

$$\mathbf{g} = \mathbf{g}_0 + \mathbf{g}_0 \mathbf{\Sigma} \mathbf{g} \tag{A13}$$

so that

$$\mathbf{g}^{-1} = \mathbf{g}_0^{-1} - \mathbf{\Sigma} = \begin{pmatrix} g_N^{-1} & -\Sigma_{NR} \\ -\Sigma_{RN} & g_R^{-1} \end{pmatrix} \tag{A14}$$

and therefore

$$\mathbf{g} = \frac{1}{\Delta} \begin{pmatrix} g_R^{-1} & \Sigma_{NR} \\ \Sigma_{RN} & g_N^{-1} \end{pmatrix}, \tag{A15}$$

where $\Delta = g_N^{-1} g_R^{-1} - \Sigma_{NR}^2$. Evidently, the matrix of propagators $\mathbf{g}$ must have poles at the dressed nucleon mass, i.e., at $\not{p} = m_N \approx 939$ MeV, and at the dressed Roper mass, i.e., at $\not{p} = m_R \approx 1365 - 95i$ MeV. Indeed, one can show that [24]

$$-\Delta = (\not{p} - m_{N0} - \tilde{\Sigma}_{NN})(\not{p} - m_{R0} - \tilde{\Sigma}_{RR}) - \tilde{\Sigma}_{NR}^2$$
$$= (\not{p} - m_{N0} - \tilde{\Sigma}_N)(\not{p} - m_{R0} - \tilde{\Sigma}_R), \tag{A16}$$

where $\tilde{\mathbf{\Sigma}} = i\mathbf{\Sigma}$, and

$$\tilde{\Sigma}_N = \frac{1}{2}\Big[m_{R0} - m_{N0} + \tilde{\Sigma}_{NN} + \tilde{\Sigma}_{RR}$$
$$- \sqrt{(m_{R0} - m_{N0} - \tilde{\Sigma}_{NN} + \tilde{\Sigma}_{RR})^2 + 4\tilde{\Sigma}_{NR}^2} \Big], \tag{A17a}$$

$$\tilde{\Sigma}_R = \frac{1}{2}\Big[m_{N0} - m_{R0} + \tilde{\Sigma}_{NN} + \tilde{\Sigma}_{RR}$$
$$+ \sqrt{(m_{R0} - m_{N0} - \tilde{\Sigma}_{NN} + \tilde{\Sigma}_{RR})^2 + 4\tilde{\Sigma}_{NR}^2} \Big] \tag{A17b}$$

are dressing amplitudes that define the "physical" nucleon and Roper propagators

$$\tilde{g}_N(p) = \frac{i}{\not{p} - m_{N0} - \tilde{\Sigma}_N + i\epsilon}, \tag{A18a}$$

$$\tilde{g}_R(p) = \frac{i}{\not{p} - m_{R0} - \tilde{\Sigma}_R + i\epsilon}. \tag{A18b}$$

One thus has that

$$\mathbf{g} = \tilde{g}_N \tilde{g}_R \begin{pmatrix} g_R^{-1} & \Sigma_{NR} \\ \Sigma_{RN} & g_N^{-1} \end{pmatrix}. \tag{A19}$$

As shown above, in the c.m. one can write

$$-i\tilde{g}_N(p) = \tilde{g}_N^+(p_0)\Lambda^+ + \tilde{g}_N^-(p_0)\Lambda^-, \tag{A20a}$$

$$-i\tilde{g}_R(p) = \tilde{g}_R^+(p_0)\Lambda^+ + \tilde{g}_R^-(p_0)\Lambda^-, \tag{A20b}$$

where $\tilde{g}_N^+(p_0)$ has a pole at $p_0 = m_N$ and $\tilde{g}_R^+(p_0)$ has a pole at $p_0 = m_R$. We can similarly write ($\alpha, \beta = N$ or R)

$$\tilde{\Sigma}_{\alpha\beta} = p_0 \gamma_0 A_{\alpha\beta} + m_N B_{\alpha\beta}$$
$$= p_0(\Lambda^+ - \Lambda^-)A_{\alpha\beta} + m_N B_{\alpha\beta}(\Lambda^+ + \Lambda^-)$$
$$= (p_0 A_{\alpha\beta} + m_N B_{\alpha\beta})\Lambda^+ - (p_0 A_{\alpha\beta} - m_N B_{\alpha\beta})\Lambda^-$$
$$\equiv \Sigma_{\alpha\beta}^+ \Lambda^+ + \Sigma_{\alpha\beta}^- \Lambda^- \tag{A21}$$

and

$$ig_\beta^{-1} = p_0 \gamma_0 - m_{\beta 0} - \tilde{\Sigma}_{\beta\beta}$$
$$= p_0(\Lambda^+ - \Lambda^-) - m_{\beta 0}(\Lambda^+ + \Lambda^-) - \tilde{\Sigma}_{\beta\beta}$$
$$= (p_0 - m_{\beta 0} - \Sigma_{\beta\beta}^+)\Lambda^+ - (p_0 + m_{\beta 0} + \Sigma_{\beta\beta}^-)\Lambda^-$$
$$\equiv [g_\beta^{-1}]^+ \Lambda^+ + [g_\beta^{-1}]^- \Lambda^-. \tag{A22}$$

It is worth noting that $[g_\beta^{-1}]^\pm = [g_\beta^\pm]^{-1}$. One can thus write in the c.m. system

$$-i\mathbf{g}(p) = \frac{1}{\Delta^+} \begin{pmatrix} [g_R^+]^{-1} & \Sigma_{NR}^+ \\ \Sigma_{RN}^+ & [g_N^+]^{-1} \end{pmatrix} \Lambda^+$$
$$+ \frac{1}{\Delta^-} \begin{pmatrix} [g_R^-]^{-1} & \Sigma_{NR}^- \\ \Sigma_{RN}^- & [g_N^-]^{-1} \end{pmatrix} \Lambda^- \tag{A23}$$
$$\equiv \mathbf{g}^+(p_0)\Lambda^+ + \mathbf{g}^-(p_0)\Lambda^-, \tag{A24}$$

where

$$\frac{1}{\Delta^\pm} = \frac{1}{[g_N^\pm]^{-1}[g_R^\pm]^{-1} - [\Sigma_{NR}^\pm]^2} = \tilde{g}_N^\pm \tilde{g}_R^\pm. \tag{A25}$$

It is evident from Eq. (A25) that the positive energy component $\mathbf{g}^+(p_0)$ has poles at $p_0 = m_N$ and $p_0 = m_R$. Moreover, the residue of $\mathbf{g}^+(p_0)$ at $p_0 = m_N$ is readily seen to be of separable form:

$$\text{Res}\,\mathbf{g}^+ = \frac{1}{\Delta^{+\prime}} \begin{pmatrix} \sqrt{[g_R^+]^{-1}} \\ \sqrt{[g_N^+]^{-1}} \end{pmatrix} \left(\sqrt{[g_R^+]^{-1}} \quad \sqrt{[g_N^+]^{-1}} \right), \tag{A26}$$

where all quantities are evaluated at $p_0 = m_N$.

APPENDIX B: The $\pi N \to \pi N$ potential

Although the $\pi N \to \pi N$ potential we have used is the same as that in [25], it is written down here in order to standardize the notation. The C's that appear in Eq. (56) are given by the expressions

$$C_1^{1/2} = -(C_{1,N} + C_{1,R}) + C_{1,\sigma\rho},$$
$$C_1^{3/2} = 2(C_{1,N} + C_{1,R}) + C_{1,\sigma\rho},$$
$$C_0^{1/2} = -(C_{0,N} + C_{0,R}) + 4(C_{0,\sigma\rho} + C_{0,\rho}),$$
$$C_0^{3/2} = 2(C_{0,N} + C_{0,R}) - 2(C_{0,\sigma\rho} + C_{0,\rho}), \tag{B1}$$

where

$$C_{0,N}(p^2) = C g_{\pi NN}^{(0)^2} h_N^2(u) \Big[\frac{1}{p^2 + m_N^2 - m_N m_\pi - 2m_\pi^2}$$
$$- \frac{(1-x_N)^2}{4m_N^2} \frac{p^2 + m_\pi^2 - m_N^2}{2p^2} \Big],$$

$$C_{0,\rho\sigma}(p^2) = -C \frac{g_{\pi NN}^{(0)^2}}{m_N} h_N^2(u) \frac{(1-x_N)^2}{4m_N} \frac{p^2 + m_\pi^2 - m_N^2}{2p^2},$$

$$C_{0,R}(p^2) = g_{\pi NR}^{(0)2} \frac{h_R^2(u)}{\sqrt{p^2}} m_\pi \Big[\frac{1}{\tilde{m}_R^2 - u} - \frac{(1-x_R)^2}{(m_N + \tilde{m}_R)^2} \Big],$$

TABLE IV. The parameters that appear only inside the potential.

	A	B
C	1.42929	1.00364
C_ρ	0.86740	0.66669

$$C_{0,\rho}(p^2) = -C_\rho \frac{g_{\pi NN}^{(0)2}}{4m_N^2} h_N^2(u) \frac{p^2 + m_\pi^2 - m_N^2}{2p^2}; \qquad (B2)$$

$$C_{1,N} = C g_{\pi NN}^{(0)2} h_N^2(u) \frac{x_N^2 - 1}{2m_N},$$

$$C_{1,\rho\sigma} = -C \frac{g_{\pi NN}^{(0)2}}{m_N} h_N^2(u) x_N^2,$$

$$C_{1,R} = g_{\pi NR}^{(0)2} h_R^2(u) \left(\frac{\tilde{m}_R - m_N}{\tilde{m}_R^2 - u} + \frac{x_R^2 - 1}{m_N + \tilde{m}_R} \right), \qquad (B3)$$

and $u = (m_N - m_\pi)^2$. Most of the parameters contained in these expressions also appear in the bare vertices and are listed in Table I. The exceptions are C and C_ρ, which are given in Table IV.

APPENDIX C: Partial wave amplitudes

To compare the $\pi N \to \pi N$ and $\gamma N \to \pi N$ amplitudes with experiment, we subject them to partial wave decompositions and then, in the case of $\pi N \to \pi N$, compute phase shifts. This appendix contains formulas for the partial wave amplitudes and phase shifts.

1. Pion-nucleon scattering

To obtain the partial wave version of $\mathcal{T}$, we first sandwich it with Dirac spinors and decompose it into isospin 1/2 and 3/2 components:

$$\mathcal{T}_{ba}^{\bar{u}u} = (P_{1/2})_{ba} \mathcal{T}_{1/2}^{\bar{u}u} + (P_{3/2})_{ba} \mathcal{T}_{3/2}^{\bar{u}u}, \qquad (C1)$$

where $\mathcal{T}_{ba}^{\bar{u}u}(k_f, p_f, k_i, p_i) = \bar{u}(\mathbf{p}_f) \mathcal{T}_{ba}(k_f, p_f, k_i, p_i) u(\mathbf{p}_i)$. When all the external particles are on shell, $k_f^2 = k_i^2 = m_\pi^2$, $p_f^2 = p_i^2 = m_N^2$, and this allows the terms on the RHS of Eq. (C1) to be expressed as

$$\mathcal{T}_t^{\bar{u}u} = \zeta_{1t} \bar{u}(\mathbf{p}_f) u(\mathbf{p}_i) + \zeta_{2t} \bar{u}(\mathbf{p}_f) \gamma_0 u(\mathbf{p}_i). \qquad (C2)$$

Calculating the partial wave amplitudes $T_{l'ljt}^{\bar{u}u}$ is then a matter of using ζ_1, ζ_2 in the following expression [51]:

$$\mathcal{T}_{l'ljt}^{\bar{u}u} = \frac{\epsilon_{\bar{k}}}{m_N} \pi \int_{-1}^{1} dx \left\{ P_l(x)[\zeta_{1t}(x) + \zeta_{2t}(x)] \right.$$
$$\left. + \left(\frac{\bar{k}}{\epsilon_{\bar{k}}} \right)^2 P_{l\pm 1}(x)[\zeta_{2t}(x) - \zeta_{1t}(x)] \right\} \delta_{l'l}, \qquad (C3)$$

where $x = \frac{\mathbf{p}_i \cdot \mathbf{p}_f}{|\mathbf{p}_i||\mathbf{p}_f|}$, $\epsilon_{\bar{k}} = \sqrt{\bar{k}^2 + m_N^2} + m_N$, and the on-shell relative momentum $\bar{k}$ is given in Eq. (82). The P's are Legendre polynomials and the $\pm$ sign refers to the total angular momentum $j = l \pm \frac{1}{2}$.

When a separable potential is used, putting the amplitude into the form of Eq. (C2) is very simple since it depends only on the total center-of-mass momentum $p = (p_0, \mathbf{0})$. In that case ζ_{1t}, ζ_{2t} are independent of x and we obtain

$$\mathcal{T}_{00\frac{1}{2}t}^{\bar{u}u} = \frac{2\pi \epsilon_{\bar{k}}}{m_N} (\zeta_{1t} + \zeta_{2t}),$$

$$\mathcal{T}_{11\frac{1}{2}t}^{\bar{u}u} = \frac{2\pi \bar{k}^2}{\epsilon_{\bar{k}} m_N} (\zeta_{2t} - \zeta_{1t}). \qquad (C4)$$

The partial wave amplitudes are related to phase shifts and the inelasticity parameter η by the formulas

$$\delta_{ljt} = \frac{1}{2} \tan^{-1} \left[\frac{-\text{Re}(\alpha \mathcal{T}_{l'ljt}^{\bar{u}u})}{\text{Im}(\alpha \mathcal{T}_{l'ljt}^{\bar{u}u}) + 1} \right], \qquad (C5)$$

$$\eta_{ljt}^2 = [1 + \text{Im}(\alpha \mathcal{T}_{l'ljt}^{\bar{u}u})]^2 + [\text{Re}(\alpha \mathcal{T}_{l'ljt}^{\bar{u}u})]^2,$$

where

$$\alpha = \frac{m_N \bar{k}}{8\pi^2 p_0}. \qquad (C6)$$

Because $\mathcal{T}_{l'ljt}^{\bar{u}u}$ has unitarity, η must be equal to 1 for all $p_0 > 0$.

2. Pion photoproduction

To compare the properly normalized $\gamma N \to \pi N$ amplitude $T_Z^{\mu a}$ with experiment, one first needs to sandwich it with Dirac spinors and isospin-$\frac{1}{2}$ states and contract it with a polarization vector:

$$M_{am_t'm_t}^{\bar{u}u}(\lambda) = \langle \tfrac{1}{2} m_t' | \bar{u}(\mathbf{p} - \mathbf{k}_f) T_Z^{\mu a}(k_f, p - k_f, p_i)$$
$$\times u(\mathbf{p}_i) | \tfrac{1}{2} m_t \rangle \hat{e}_\mu(\lambda), \qquad (C7)$$

where m_t and m_t' are the z-axis projections of the initial and final nucleon isospins. The polarization vector is given by

$$\hat{e}_\mu(\pm 1) = \mp \frac{1}{\sqrt{2}}(0, 1, \pm i, 0), \qquad (C8)$$

where the argument $\lambda = \pm 1$ is the helicity; the amplitudes we calculate are independent of how this is chosen. When the kinematics are set according to Eq. (81), $M_{am_t'm_t}^{\bar{u}u}(\lambda)$ can be decomposed into products of ordinary numbers and rotationally invariant matrices as [52]

$$-\frac{m_N}{4\pi p_0} M_{am_t'm_t}^{\bar{u}u}(\lambda) = i\boldsymbol{\sigma} \cdot \hat{\mathbf{e}}(\lambda) J_{am_t'm_t}^{(1)}$$
$$+ \boldsymbol{\sigma} \cdot \hat{\mathbf{k}}_f \boldsymbol{\sigma} \cdot [\hat{\mathbf{q}} \times \hat{\mathbf{e}}(\lambda)] J_{am_t'm_t}^{(2)} \qquad (C9)$$
$$+ i\boldsymbol{\sigma} \cdot \hat{\mathbf{q}} \hat{\mathbf{k}}_f \cdot \hat{\mathbf{e}}(\lambda) J_{am_t'm_t}^{(3)}$$
$$+ i\boldsymbol{\sigma} \cdot \hat{\mathbf{k}}_f \hat{\mathbf{k}}_f \cdot \hat{\mathbf{e}}(\lambda) J_{am_t'm_t}^{(4)},$$

where $\hat{\mathbf{k}}_f = \frac{\mathbf{k}_f}{|\mathbf{k}_f|}$ and $\hat{\mathbf{q}} = \frac{\mathbf{q}}{|\mathbf{q}|}$. In writing this it has been assumed that $\bar{u}$ and u have the Bjorken and Drell [53] normalization.

Note that the LHS of Eq. (C9) differs from Eq. (B.4) of Nozawa, Blankleider, and Lee (NBL) [3] by a factor of -1. This discrepancy occurs because NBL's amplitude $M_{\pi N, \gamma N}^a$ consists of Feynman diagrams multiplied by $-i$. This may be seen by deriving the Born terms in their Eqs. (2.8b) and (2.8c)

from Feynman rules. Meanwhile, the amplitude $M_{am'_t m_t}^{\bar{u}u}$ in the above Eq. (C9) consists of Feynman diagrams multiplied by i and some renormalization constants. To compensate, an extra minus sign has been included in this equation.

$J_{am'_t m_t}^{(1)}$, $J_{am'_t m_t}^{(2)}$, etc. are used to calculate the invariant amplitudes,

$$
\begin{pmatrix} E_{l+}^{am'_t m_t} \\ E_{l-}^{am'_t m_t} \\ M_{l+}^{am'_t m_t} \\ M_{l-}^{am'_t m_t} \end{pmatrix} = \int_{-1}^{1} dx\, D_l(x) \begin{pmatrix} J_{am'_t m_t}^{(1)} \\ J_{am'_t m_t}^{(2)} \\ J_{am'_t m_t}^{(3)} \\ J_{am'_t m_t}^{(4)} \end{pmatrix}, \tag{C10}
$$

where $x = \cos\theta$ and θ is the same as that which appears in Eq. (81). The matrix D_l is given by

$$
D_l(x) = \begin{pmatrix} a_l P_l & -a_l P_{l+1} & \frac{a_l l}{2l+1} Q_l & \frac{a_l(l+1)}{2l+3} Q_{l+1} \\ b_l P_l & -b_l P_{l-1} & -\frac{b_l(l+1)}{2l+1} Q_l & -\frac{b_l l}{2l-1} Q_{l-1} \\ c_l P_l & -c_l P_{l+1} & -\frac{c_l}{2l+1} Q_l & 0 \\ -d_l P_l & d_l P_{l-1} & \frac{d_l}{2l+1} Q_l & 0 \end{pmatrix}, \tag{C11}
$$

where $a_l = \frac{1}{2(l+1)}$, $b_l = \frac{1}{2l}$, $c_l = \frac{1}{2(l+1)}$, $d_l = \frac{1}{2l}$, $Q_l = P_{l-1} - P_{l+1}$. The P's in Eq. (C11) and in Q are Legendre polynomials and are functions of x.

Assuming the charged pion isospin matrices use the sign and normalization convention $\tau_{\pm 1} \equiv (\tau_1 \pm i\tau_2)/\sqrt{2}$ and $\tau_0 \equiv \tau_3$, the multipole amplitudes are given by the following combinations of physical amplitudes [54]:

$$
M_{l\pm}(0) = \frac{1}{2\sqrt{2}} [M_{l\pm}(\gamma n \to \pi^- p) + M_{l\pm}(\gamma p \to \pi^+ n)],
$$

$$
M_{l\pm}(1/2) = M_{l\pm}(\gamma p \to \pi^0 p) - \frac{1}{2\sqrt{2}} [3M_{l\pm}(\gamma n \to \pi^- p) - M_{l\pm}(\gamma p \to \pi^+ n)], \tag{C12}
$$

where $M_{l\pm}(\gamma n \to \pi^- p)$ is equal to $M_{l\pm}^{am'_t m_t}$ with $a = -1$, $m'_t = \frac{1}{2}$, $m_t = -\frac{1}{2}$. Similarly, $M_{l\pm}(\gamma p \to \pi^+ n)$ is equal to $M_{l\pm}^{am'_t m_t}$ with $a = 1$, $m'_t = -\frac{1}{2}$, $m_t = \frac{1}{2}$ and $M_{l\pm}(\gamma p \to \pi^0 p)$ is equal to $M_{l\pm}^{am'_t m_t}$ with $a = 0$, $m'_t = \frac{1}{2}$, $m_t = \frac{1}{2}$. It is also conventional to decompose the $t = 1/2$ amplitudes into "proton" and "neutron" pieces:

$$
{}_p M_{l\pm}(1/2) = M_{l\pm}(0) + \frac{1}{3} M_{l\pm}(1/2),
$$

$$
{}_n M_{l\pm}(1/2) = M_{l\pm}(0) - \frac{1}{3} M_{l\pm}(1/2). \tag{C13}
$$

Relations identical to those appearing in Eqs. (C12) and (C13) also apply to the E amplitudes. To check for mistakes in the computer program used to calculate the multipole amplitudes, we verified that it correctly reproduces the Born term results of Laget [55].

APPENDIX D: THE COUPLING CONSTANT

To evaluate the coupling constant of the dressed πNN vertices, we compare the pole (second) term from the first of Eqs. (33) to a similar diagram that has bare vertices with $g_{\pi NN}$

substituted for $g_{\pi NN}^{(0)}$ and a bare propagator for a physical mass nucleon. The dressed coupling constant may be extracted by equating the residues of the two diagrams at the nucleon pole.

The properly normalized $\pi N \to \pi N$ pole term is

$$
\mathcal{T}_{\text{Pole}}(k_f, p_f, k_i, p_i) = iZ_2 \boldsymbol{f}(k_f, p_f, p)\boldsymbol{g}(p)\bar{\boldsymbol{f}}(k_i, p, p_i), \tag{D1}
$$

where $p = p_i + k_i = p_f + k_f = (p_0, \mathbf{0})$. Putting the external particles on shell (that is, choosing $p_i^2 = p_f^2 = m_N^2$, $k_i^2 = k_f^2 = m_\pi^2$) and sandwiching $\mathcal{T}_{\text{Pole}}$ with Dirac spinors allows it to be expressed in terms of the $\Lambda^\pm$ operators, giving

$$
\mathcal{T}_{\text{Pole}}^{\bar{u}u} = \mathcal{T}_{\text{Pole}}^+ U^+ + \mathcal{T}_{\text{Pole}}^- U^-, \tag{D2}
$$

where $\mathcal{T}_{\text{Pole}}^{\bar{u}u} = \bar{u}(\mathbf{p}_f)\mathcal{T}_{\text{Pole}} u(\mathbf{p}_i)$ and

$$
T_{\text{Pole}}^\pm(p_0) = -I_\tau Z_2 \sum_{\beta\alpha} f_\beta^\mp(p_0) g_{\beta\alpha}^\mp(p_0) \bar{f}_\alpha^\mp(p_0),
$$

$$
U^\pm = \bar{u}(\mathbf{p}_f)\Lambda^\pm u(\mathbf{p}_i). \tag{D3}
$$

The $f_\alpha^\pm(p_0)$ factors are ordinary numbers (not matrices) given by expressions that are straightforward to derive, while I_τ is an isospin factor. Now, the negative energy propagator $\boldsymbol{g}^-$ does not have poles at the particle masses and so the residue of $\mathcal{T}_{\text{Pole}}$ at $p_0 = m_N$ is

$$
\operatorname*{Res}_{p_0 = m_N} \mathcal{T}_{\text{Pole}}^{\bar{u}u} = -I_\tau Z_2 \sum_{\alpha\beta} f_\alpha^+(m_N) f_\beta^+(m_N) \sqrt{Z_\alpha Z_\beta}\, U^-. \tag{D4}
$$

The diagram to which this should be compared is

$$
V_{\text{Pole}}^{\bar{u}u} = -I_\tau g_{\pi NN}^2 \bar{u}(\mathbf{p}_f)\gamma_5 \frac{\not{p} + m_N}{p^2 - m_N^2 + i\epsilon} \gamma_5 u(\mathbf{p}_i) \tag{D5}
$$

When all particles are on shell and the diagram is multiplied by Dirac spinors, pseudovector coupling is equivalent to pseudoscalar. Using pseudoscalar coupling therefore causes no loss of generality, and in either case the residue at $p_0 = m_N$ is

$$
\operatorname*{Res}_{P_0 = m_N} V_{\text{Pole}}^{\bar{u}u} = -I_\tau g_{\pi NN}^2 U^-. \tag{D6}
$$

Equating this to the RHS of Eq. (D4), we see that

$$
g_{\pi NN} = \sqrt{Z_2} f_N^+(m_N)\sqrt{Z_N} + \sqrt{Z_2} f_R^+(m_N)\sqrt{Z_R}. \tag{D7}
$$

The bare coupling constant $g_{\pi NN}^{(0)}$ should be set so that $g_{\pi NN} \approx 13.02$.

[1] E. Klempt and J.-M. Richard, Rev. Mod. Phys. **82**, 1095 (2010).

[2] L. Tiator, D. Drechsel, S. S. Kamalov, and M. Vanderhaeghen, Eur. Phys. J. Spec. Top. **198**, 141 (2011).

[3] S. Nozawa, B. Blankleider, and T. S. H. Lee, Nucl. Phys. A **513**, 459 (1990).

[4] T. S. H. Lee and B. C. Pearce, Nucl. Phys. A **530**, 532 (1991).

[5] Y. Surya and F. Gross, Phys. Rev. C **53**, 2422 (1996).

[6] V. Pascalutsa and J. A. Tjon, Phys. Rev. C **70**, 035209 (2004).

[7] A. Matsuyama, T. Sato, and T. S. H. Lee, Phys. Rept. **439**, 193 (2007).

[8] B. Julia-Diaz, T. S. H. Lee, A. Matsuyama, T. Sato, and L. C. Smith, Phys. Rev. C **77**, 045205 (2008).

[9] Y. Takahashi, Nuovo Cimento **6**, 371 (1957).

[10] W. Bentz, Nucl. Phys. A **446**, 678 (1985).

[11] A. N. Kvinikhidze and B. Blankleider, invited talk given at the Joint Japan Australia Workshop: Quarks, Hadrons and Nuclei, Adelaide, November 15–24, 1995 (unpublished).

[12] H. Haberzettl, Phys. Rev. C **56**, 2041 (1997).

[13] A. N. Kvinikhidze and B. Blankleider, Phys. Rev. C **56**, 2963 (1997).

[14] A. N. Kvinikhidze and B. Blankleider, Nucl. Phys. A **631**, 559c (1998).

[15] A. N. Kvinikhidze and B. Blankleider, Phys. Rev. C **60**, 044003 (1999).

[16] F. Gross, A. Stadler, and M. T. Pena, Phys. Rev. C **69**, 034007 (2004).

[17] T. Sato and T. S. H. Lee, J. Phys. G **36**, 073001 (2009).

[18] H. Haberzettl, K. Nakayama, and S. Krewald, Phys. Rev. C **74**, 045202 (2006).

[19] F. Huang, M. Doring, H. Haberzettl, J. Haidenbauer, C. Hanhart *et al.*, in *The 8th International Workshop on the Physics of Excited Nucleons: NSTAR 2011*, edited by V. Burkert, M. Jones, M. Pennington, and D. Richards, AIP Conf. Proc. No. 1432 (AIP, New York, 2012), p. 319.

[20] F. Huang, M. Doring, H. Haberzettl, J. Haidenbauer, C. Hanhart, S. Krewald, U. G. Meissner, and K. Nakayama, Phys. Rev. C **85**, 054003 (2012).

[21] J. S. Ball and T.-W. Chiu, Phys. Rev. D **22**, 2550 (1980) **[23**, 3085(E) (1981)].

[22] J. S. Ball and T.-W. Chiu, Phys. Rev. D **22**, 2542 (1980).

[23] M. E. Peskin and D. V. Schroeder, *An Introduction to Quantum Field Theory* (Westview, Boulder, CO, 1995).

[24] B. C. Pearce and I. R. Afnan, Phys. Rev. C **34**, 991 (1986).

[25] F. Gross and Y. Surya, Phys. Rev. C **47**, 703 (1993).

[26] B. C. Pearce and I. R. Afnan, Phys. Rev. C **30**, 2022 (1984).

[27] I. R. Afnan, Austral. J. Phys. **44**, 201 (1991).

[28] SAID Partial-Wave Analysis Facility, Data Analysis Center, Institute of Nuclear Studies, GWU, 2018, http://gwdac.phys.gwu.edu.

[29] C. H. M. van Antwerpen, A gauge invariant unitary theory for pion photoproduction, Ph.D. thesis, Flinders University, 1994 (unpublished).

[30] C. H. M. van Antwerpen and I. R. Afnan, Phys. Rev. C **52**, 554 (1995).

[31] F. Gross and D. O. Riska, Phys. Rev. C **36**, 1928 (1987).

[32] L. E. Price, J. R. Dunning, M. Goitein, K. Hanson, T. Kirk, and R. Wilson, Phys. Rev. D **4**, 45 (1971).

[33] C. Herberg *et al.*, Eur. Phys. J. A **5**, 131 (1999).

[34] I. Passchier, R. Alarcon, T. S. Bauer, D. Boersma, J. F. J. van den Brand, L. D. van Buuren, H. J. Bulten, M. Ferro-Luzzi, P. Heimberg, D. W. Higinbotham, C. W. de Jager, S. Klous, H. Kolster, J. Lang, B. L. Militsyn, D. Nikolenko, G. J. L. Nooren, B. E. Norum, H. R. Poolman, I. Rachek, M. C. Simani, E. Six, D. Szczerba, H. de Vries, K. Wang, and Z.-L. Zhou, Phys. Rev. Lett. **82**, 4988 (1999).

[35] P. Markowitz, J. M. Finn, B. D. Anderson, H. Arenhövel, A. R. Baldwin, D. Barkhuff, K. B. Beard, W. Bertozzi, J. M. Cameron, C. C. Chang, G. W. Dodson, K. Dow, T. Eden, M. Farkhondeh, B. Flanders, C. Hyde-Wright, W.-D. Jiang, D. Keane, J. J. Kelly, W. Korsch, S. Kowalski, R. Lourie, R. Madey, D. M. Manley, J. Mougey, B. Ni, T. Payerle, P. Pella, T. Reichelt, P. M. Rutt, M. Spraker, D. Tieger, W. Turchinetz, P. E. Ulmer, S. Van Verst, J. W. Watson, L. B. Weinstein, R. R. Whitney, and W. M. Zhang, Phys. Rev. C **48**, R5 (1993).

[36] E. E. W. Bruins, T. S. Bauer, H. W. den Bok, C. P. Duif, W. C. van Hoek, D. J. J. de Lange, A. Misiejuk, Z. Papandreou, E. P. Sichtermann, J. A. Tjon, H. W. Willering, D. M. Yeomans, H. Reike, D. Durek, F. Frommberger, R. Gothe, D. Jakob, G. Kranefeld, C. Kunz, N. Leiendecker, G. Pfeiffer, H. Putsch, T. Reichelt, B. Schoch, D. Wacker, D. Wehrmeister, M. Wilhelm, E. Jans, J. Konijn, R. de Vries, C. Furget, E. Voutier, and H. Arenhövel, Phys. Rev. Lett. **75**, 21 (1995).

[37] A. W. Thomas and W. Weise, *The Structure of the Nucleon* (Wiley-VCH, Wennheim, 2001).

[38] F. Iachello, A. Jackson, and A. Lande, Phys. Lett. B **43**, 191 (1973).

[39] R. Bijker and F. Iachello, Phys. Rev. C **69**, 068201 (2004).

[40] E. M. Nyman, Nucl. Phys. A **154**, 97 (1970).

[41] M. Hare, Ann. Phys. (NY) **74**, 595 (1972).

[42] M. Göckeler, T. R. Hemmert, R. Horsley, D. Pleiter, P. E. L. Rakow, A. Schafer, and G. Schierholz, Phys. Rev. D **71**, 034508 (2005).

[43] C. Alexandrou, M. Brinet, J. Carbonell, M. Constantinou, P. A. Harraud, P. Guichon, K. Jansen, T. Korzec, and M. Papinutto, Phys. Rev. D **83**, 094502 (2011).

[44] G. A. Miller, Phys. Rev. C **66**, 032201 (2002).

[45] J. C. R. Bloch, C. D. Roberts, S. M. Schmidt, A. Bender, and M. R. Frank, Phys. Rev. C **60**, 062201 (1999).

[46] G. Eichmann, Phys. Rev. D **84**, 014014 (2011).

[47] B. Kubis and U.-G. Meissner, Nucl. Phys. A **679**, 698 (2001).

[48] T. Fuchs, J. Gegelia, and S. Scherer, J. Phys. G **30**, 1407 (2004).

[49] M. R. Schindler, J. Gegelia, and S. Scherer, Eur. Phys. J. A **26**, 1 (2005).

[50] A. D. Lahiff, Covariant formulation of pion-nucleon scattering, Ph.D. thesis, Flinders University, 1999.

[51] A. D. Lahiff and I. R. Afnan, Phys. Rev. C **60**, 024608 (1999).

[52] G. F. Chew, M. L. Goldberger, F. E. Low, and Y. Nambu, Phys. Rev. **106**, 1345 (1957).

[53] J. D. Bjorken and S. D. Drell, in *Relativistic Quantum Mechanics*, International Series in Pure and Applied Physics (McGraw-Hill, New York, 1964).

[54] W. Pfeil and D. Schwela, Nucl. Phys. B **45**, 379 (1972).

[55] J. Laget, Phys. Rep. **69**, 1 (1981).